Published in "Journal of Biological Chemistry
doi: 10.1074/jbc.M112.400564 jbc.M112.400564 , 2012"
which should be cited to refer to this work.

Yeast ribosomal protein L40 assembles late into pre-60S ribosomes and is required for their cytoplasmic maturation

Antonio Fernández-Pevida[1], Olga Rodríguez-Galán[1], Antonio Díaz-Quintana[2], Dieter Kressler[3] and Jesús de la Cruz[1]

[1]From the Departamento de Genética, Universidad de Sevilla, E-41012 Sevilla, Spain, [2]Instituto de Bioquímica Vegetal y Fotosíntesis, Universidad de Sevilla-CSIC, E-41092 Sevilla, Spain and [3]Department of Biology, Unit of Biochemistry, University of Fribourg, CH-1700 Fribourg, Switzerland.

Running title: *Role of L40 in yeast ribosome synthesis and function*

To whom correspondence should be addressed: Jesús de la Cruz, Departamento de Genética, Facultad de Biología, Universidad de Sevilla. Avda. de la Reina Mercedes, 6; E-41012 Sevilla, SPAIN. Phone: +34 95 455 71 06; Fax: +34 95 455 71 04; E-mail: jdlcd@us.es

Keywords: Ribosome biogenesis, pre-rRNA processing, RNA, nucleolus, affinity purification, ubiquitin, yeast.

Background: The contribution of ribosomal proteins to ribosome assembly and function is often not well understood.
Results: L40 assembles within the cytoplasm into pre-60S subunits and is required for Nmd3 and Rlp24 recycling.
Conclusion: L40 contributes to formation of 60S subunits competent for subunit joining and translation elongation.
Significance: Our analysis of L40 function reveals an additional step during cytoplasmic pre-60S maturation events.

SUMMARY

Most ribosomal proteins play important roles in ribosome biogenesis and function. Herein, we have examined the contribution of the essential ribosomal protein L40 in these processes in the yeast *Saccharomyces cerevisiae*. Deletion of either the *RPL40A* or *RPL40B* gene and *in vivo* depletion of L40 impair 60S ribosomal subunit biogenesis. Polysome profile analyses reveal the accumulation of half-mers and a moderate reduction in free 60S ribosomal subunits. Pulse-chase, northern blotting and primer extension analyses in the L40-depleted strain clearly indicate that L40 is not strictly required for the pre-rRNA processing reactions but contributes to optimal 27SB pre-rRNA maturation. Moreover, depletion of L40 hinders the nucleo-cytoplasmic export of pre-60S ribosomal particles. Importantly, all these defects most likely appear as the direct consequence of impaired Nmd3 and Rlp24 release from cytoplasmic pre-60S ribosomal subunits and their inefficient recycling back into the nucle(ol)us. In agreement, we show that hemagglutinin epitope-tagged L40A assembles in the cytoplasm into almost mature pre-60S ribosomal particles. Finally, we have identified that the hemagglutinin epitope-tagged L40A confers resistance to sordarin, a translation inhibitor that impairs the function of eukaryotic elongation factor 2, while the *rpl40a* and *rpl40b* null mutants are hypersensitive to this antibiotic. We conclude that L40 is assembled at a very late stage into pre-60S ribosomal subunits and that its incorporation into 60S ribosomal subunits is a prerequisite for subunit joining and may ensure proper functioning of the translocation process.

Ribosomes are the huge ribonucleoprotein particles that catalyse protein synthesis. In all organisms, ribosomes are composed of two ribosomal subunits (r-subunits), the large one about twice the size of the small one (1). Over the last decade, the atomic structures of the small and large r-subunits have been determined from bacteria, archaea and more recently from eukaryotes (2-14). These results have confirmed the long-thought suggestion that the eukaryotic cytoplasmic ribosomes display considerable structural and functional similarities to their prokaryotic counterparts but are significantly larger and more complex (15,16).

In eukaryotes, the synthesis of cytoplasmic ribosomes is a compartmentalised process that takes place largely in the nucleolus (reviewed in (17-19)) although late steps occur in the nucleoplasm and even in the cytoplasm

(reviewed in (20)). Ribosome biogenesis is evolutionary conserved throughout eukaryotes (21,22), but it has been best studied in the yeast *Saccharomyces cerevisiae* (23). In the yeast nucleolus, the mature 18S, 5.8S and 25S rRNAs are co-transcribed as a single large precursor rRNA (pre-rRNA) by RNA polymerase I whereas the pre-5S rRNA is independently transcribed by RNA polymerase III (24). The yeast pre-rRNA processing pathway is currently almost fully known and requires a series of sequential endo- and exonucleolytic reactions (**Fig. S1**). Pre-rRNA processing occurs concomitantly to most rRNA modification reactions, folding of pre-rRNAs and assembly of most r-proteins to form pre-ribosomal particles (**Fig. S2**). Late pre-ribosomal particles are exported to the cytoplasm where they undergo final maturation (**Fig. S2**). It has been shown that more than 250 non-ribosomal protein factors and 75 small nucleolar RNAs are involved in ribosome synthesis. All these factors, whose precise functions remain largely unknown, likely allow the ribosome maturation process to proceed with the required speed, accuracy and directionality (25-27).

Ribosomal proteins are critically required for translation, most likely due to their role in directing the folding and maintaining the structure of the ribosome (e.g. (28-32)). Moreover, r-proteins are the binding sites for translation factors, ribosome-associated chaperones, the signal recognition particle and the translocon (e.g., (33-37)); they can be targets for translation regulatory events (38,39) and antibiotics (40,41); some r-proteins have even extra-ribosomal roles (42-46). The consequences on ribosome biogenesis due to loss-of-function of most of the essential yeast r-protein genes has been reported (47,48). One of the current challenges of the ribosome biogenesis field is defining the course of the assembly of r-proteins at a satisfactorily high resolution. A rough picture of this pathway has been obtained by pioneer work in yeast and HeLa cells (49,50). These studies indicate that most r-proteins are incorporated into nuclear pre-ribosomal particles either early or late in the process. Few r-proteins were found to assemble in the cytoplasm. These results are consistent with the compositional analyses of early and late pre-ribosomal complexes purified by the tandem affinity purification (TAP) method (e.g. (51-53)) and the specific study of the incorporation of tagged 40S r-proteins into 90S and 43S pre-ribosomal particles (54). An equivalent study of the incorporation of 60S r-proteins into pre-60S r-particles has not yet been reported. There is only information on the timing of assembly for few 60S r-proteins, such as L5 and L11 (55), L10 (56), L17 (57), L24 (58), L26 (59), L35 (60) and P0 (61).

We are interested in understanding the contribution of specific 60S r-proteins to ribosome biogenesis and function (e.g. (59-62)). In this study, we have undertaken the functional analysis of L40 in yeast ribosome synthesis. Homologues of L40 are found in archaea (archaeal L40e) but not in bacteria (63,64). Interestingly, eukaryotic L40 is generated by proteolytic cleavage of a hybrid protein (Ubi1 or Ubi2), in which ubiquitin is fused to the N-terminus of L40 (65,66). There is another eukaryotic r-protein, S27a (yeast S31), which is synthesized as an ubiquitin-fusion precursor protein (yeast Ubi3) (65,66). The role of the ubiquitin moiety of yeast Ubi3 has been addressed (66,67), however, that of Ubi1 and Ubi2 remains unexplored. Herein, we show that depletion of L40 leads to a mild 27SB and 7S pre-rRNA processing delay and a nuclear retention of pre-60S r-particles. Although depletion of L40 barely affects the net production of 60S r-subunits, polysome profile analyses reveal a strong accumulation of half-mers. Noteworthy, we show that L40 assembles predominantly into cytoplasmic pre-60S r-particles. The incorporation of L40 is a prerequisite for the release, and hence the subsequent recycling back into the nucle(ol)us, of Nmd3 and Rlp24 from cytoplasmic pre-60S particles. Finally, we have monitored how L40 may influence the ribosome function during translation. Interestingly, *rpl40a* or *rpl40b* null mutants are hypersensitive to the antifungal sordarin derivative GM193663, while a HA-tagged L40 construct confers resistance to this antibiotic. Sordarin is a fungal specific protein synthesis inhibitor that impairs the function of eukaryotic elongation factor 2 (eEF2) (68-70). Altogether, these data indicate that L40 is required for the ribosomal subunit joining process; moreover, L40 might be involved in the recruitment of the translation elongation factor eEF2 and thereby contributing to the proper functioning of the ribosomal translocation process.

EXPERIMENTAL PROCEDURES

Strains and microbiological methods — The yeast strains used in this study are listed in **Table S1**. Strain JDY919 was generated by PCR-based gene disruption of the *RPL40A* gene in the W303 strain. To this end, we used plasmid

pFA6a, which contains the kanMX4 module, as a template (71) and the oligonucleotide pair RPL40A-kanUP/RPL40A-kanDOWN (**Table S2**). After transformation with the PCR product and selection of G418 resistant colonies, disruption was confirmed by PCR analysis on genomic DNA of several candidates with oligonucleotides RPL40A UP/DOWN. Strain JDY920 is a *rpl40a*::kanMX4 meiotic segregant of JDY919. To obtain strain JDY922, which is a *rpl40b*::kanMX4 meiotic segregant of JDY921, we followed a similar approach. First, we obtained diploid JDY921 by PCR-based gene disruption of the *RPL40B* gene in the W303 strain. In this case, oligonucleotides RPL40B-kanUP/RPL40B-kanDOWN (**Table S2**) were used to amplify the kanMX4 module of plasmid pFA6a and oligonucleotides RPL40B-UP/RPL40B-DOWN (**Table S2**) to confirm the disruption by PCR. Strain JDY711 is a *rpl35b*::kanMX4 mutant that was obtained by introducing this mutation from RBY139 (60) into the W303 background by three subsequent back-crosses with W303-1B.

Growth and handling of yeast and media followed standard procedures (72). Yeast cells were grown at 30 ºC either in rich medium (1% yeast extract, 2% peptone) or in minimal medium (0.15% yeast nitrogen base, 0.5% ammonium sulphate) supplemented with the appropriate amino acids and bases as nutritional requirements and containing either 2% galactose (YPGal, SGal) or 2% glucose (YPD, SD). To prepare plates, 2% agar was added to the media before sterilisation. When required, antibiotics were also added at the indicated concentration. Tetrad dissections were performed using a Singer MS micromanipulator. *Escherichia coli* DH5α strain was used for common cloning and propagation of plasmids (73).

Plasmids — The plasmids used in this study are listed in **Table S3**. To generate YCplac33-RPL40A and YCplac111-RPL40A, a PCR was performed using yeast genomic DNA as template and the oligonucleotides RPL40A-UP and RPL40A-DOWN (**Table S2**), placed plus-minus 1 kb upstream and downstream from the start-stop codon of the *UBI1* ORF, respectively. The *ca*. 2.8 kb PCR product was cloned into pGEM®-T Easy (Promega), then restricted with *Eco*RI and *Pst*I and cloned into YCplac33 and YCplac111 (74), which were also digested with the same enzymes. To generate YCplac33-RPL40B and YCplac111-RPL40B, we followed a similar strategy using the oligonucleotide pair RPL40B-UP/RPL40B-DOWN (**Table S2**). In this case, *Bam*HI was used to subclone a *ca.* 2.8 kb fragment from pGEM®-T Easy into YCplac33 and YCplac111. The resulting plasmids, whose correctness was confirmed by DNA sequencing, complemented both the *rpl40a* and *rpl40b* null alleles to the wild-type extent (see **Fig. S3-4**).

To construct pAS24-RPL40A, a *ca.* 1.8 kb PCR product containing the *UBI1* coding region and its intron was obtained by PCR using yeast genomic DNA as template and the GAL-RPL40A-UP and GAL-RPL40A-DOWN primers (**Table S2**). This product was cloned into pGEM®-T Easy, then restricted with *Sal*I and *Pst*I and cloned into pAS24 (75), which was also digested with the same enzymes. The resulting plasmid, whose correctness was confirmed by DNA sequencing, complemented the *rpl40* null strain to the wild-type extent in galactose containing media (see **Fig. 2**).

Plasmid YCplac33-UB-HA-RPL40A was generated by PCR using yeast genomic DNA as template and the oligonucleotide pairs HA-RPL40A-P1/HA-RPL40A-P2 and HA-RPL40A-P3/HA-RPL40A-P4. The corresponding PCR products P12 and P34 were cloned into pGEM®-T Easy. Fragment P12 was digested with *Eco*RI and *Kpn*I and cloned into *Eco*RI/*Kpn*I-restricted YCplac33 to generate YCplac33-P12. Then, the fragment P34 was digested with *Kpn*I and *Pst*I and cloned into *Kpn*I/*Pst*I-restricted YCplac33-P12. The resulting plasmid, whose correctness was confirmed by DNA sequencing, partially complemented the *rpl40* null (see **Fig. S5**). YCplac111-UB-HA-RPL40A was constructed by using a similar approach.

To generate YCplac33-RLP24-GFP, a PCR was performed using yeast genomic DNA as template and the oligonucleotides RLP24GFP-UP and RLP24GFP-DOWN (**Table S2**), placed 1 kb upstream from the start codon of the *RLP24* ORF and replacing the *RLP24* stop codon with a *Bam*HI restriction site respectively. The *ca*. 1.6 kb PCR product was cloned into pGEM®-T (Promega), then excised with *Eco*RI and *Bam*HI and cloned into YCplac33-yeGFP/TCYC1 (76), which was also digested with the same enzymes.

Construction of a GAL::RPL40 allele and in vivo depletion of L40 — Strain JDY920 harbouring the YCplac33-RPL40A plasmid was crossed to JDY923, which is a *MAT*α *rpl40b::*kanMX4 segregant of JDY921. The resulting diploid was sporulated and tetrads were dissected. G418-resistant spore clones from at least three complete non-parental ditypes were transformed with pAS24-RPL40A, which allows expression of Ubi1 under the control of a *GAL*

promoter. Transformants were streaked on SGal-Leu plates and subjected to plasmid shuffling on 5-FOA-containing SGal plates at 30 ºC. One of these clones, JDY925 [pAS24-RPL40A], which we named the *GAL::RPL40* strain, was used for further work.

For *in vivo* depletion of L40, the *GAL::RPL40* strain was grown in liquid YPGal medium at 30 ºC until mid-exponential phase (OD_{600} = 0.8), and then harvested, washed and transferred to liquid YPD medium. Cell growth was monitored over a period of 24 h, during which the cultures were regularly diluted into fresh YPD medium. As control, the wild-type W303-1A strain was used. At different time points, samples were collected to perform protein and RNA extractions, and polysome analysis.

Sucrose gradient centrifugation — Cell extracts for polysome and r-subunit analyses were prepared and analysed as previously described (77) using an ISCO UA-6 system equipped to continuously monitor A_{254}.

Protein extractions and western blotting analyses — Total yeast protein extracts were prepared and analysed by western blotting according to standard procedures (73). The following primary antibodies were used: mouse monoclonal anti-HA (HA.11 16B12, Covance), mouse monoclonal anti-Nop1 (MCA-28F2, EnCor Biotechnology), mouse monoclonal anti-GFP (Roche), mouse monoclonal BH5 anti-stalk r-proteins (a gift from J. P. G. Ballesta) (78), mouse monoclonal anti-L3 (a gift from J. R. Warner) (42), mouse monoclonal 3AG10 anti-L12 (a gift from J. P. G. Ballesta) (79), rabbit polyclonal anti-L1 (a gift from F. Lacroute) (80), rabbit polyclonal anti-L5 (a gift from S.R. Valentini) (81), rabbit polyclonal anti-L10 (a gift from B. L. Trumpower) (82), rabbit polyclonal anti-L35 (a gift from M. Seedorf) (83), rabbit polyclonal anti-Mrt4 (a gift from J. P. G. Ballesta) (79) and rabbit polyclonal anti-Has1 (a gift from P. Linder) (84). Goat anti-rabbit or anti-mouse horseradish peroxidase-conjugated antibodies (Bio-Rad) were used as secondary antibodies. Immune complexes were visualized using an enhanced chemiluminescence detection kit (Pierce).

RNA analyses — RNA extraction, northern hybridisation and primer extension analyses were carried out according to standard procedures (85,86). In all experiments, RNA was extracted from samples corresponding to 10 OD_{600} units of exponentially grown cells. Equal amounts of total RNA was loaded on gels or used for primer extension reactions (86). The sequences of oligonucleotides used for northern hybridisation and primer extension analyses have been described previously (87) and are listed in **Table S2**. Phosphorimager analysis was performed in a FLA-5100 imaging system (Fujifilm).

Pulse-chase labelling of pre-rRNA was performed exactly as described previously (88), using 100 mCi of [5,6-^{3}H]uracil (Perkin Elmer; 45 to 50 Ci/mmol) per 40 OD_{600} of yeast cells. Both the wild-type and *GAL::RPL40* strains were first transformed with an empty YCplac33 plasmid to make them prototrophic for uracil. Then, they were pre-grown in liquid SGal-Ura medium and shifted to liquid SD-Ura for 12 h. At this time point, the *GAL::RPL40* strain was doubling every *ca.* 10-12 h compared with *ca.* 2 h for the wild-type strain. The cells were pulse-labelled for 2 min, then chased for 5, 15, 30 and 60 min with a large excess of non-radioactive uracil. Total RNA was extracted as above and 20,000 c.p.m. per RNA sample was loaded on gels and analysed as described in (88).

Immunoprecipitation of the HA-L40A protein — For immunoprecipitation experiments, 150 ml of HA-tagged or untagged negative control cells were grown in YPD medium to an OD_{600} of 0.8, washed with cold water, harvested and concentrated in 500 µl of ice-cold HA lysis buffer [50 mM Tris-HCl, pH7.5; 5 mM $(CH_3COO)_2Mg$; 150 mM KCl; 0.2% Triton X-100] containing a protease inhibitor cocktail (Complete, Roche) and 1 mM PMSF. Cells were disrupted by vigorous shaking with glass beads in a Fastprep®-24 (MP Biomedicals) at 4ºC and total cell extracts were obtained by centrifugation in a microfuge at the maximum speed (*ca.* 16,100 x *g*) for 15 min at 4 ºC. About 10% and 2% of the resulting supernatants were taken to analyse total RNA and protein, respectively. To the rest (about 450 µl), 2.5 µg of rat anti-HA High Affinity antibody (Roche) was added and the mixture was incubated for 1 h at 4ºC with end-over-end tube rotation. Then, 100 µl of Protein A Sepharose beads (GE Healthcare) were added and the new mixture was incubated with end-over-end tube rotation for 4 h at 4 ºC. After incubation, the beads were washed seven times with 1 ml of the HA lysis buffer at 4 ºC and finally collected. Protein was extracted with Laemmli buffer from both total cell extract samples and 1/10th of the beads. The extracted proteins were analysed by western blotting using mouse monoclonal anti-HA antibody (HA.11 16B12, Covance). RNA was extracted from the total cell extract samples and the rest of the beads as exactly described in (89).

The extracted RNA was analysed by northern blotting as above described.

Affinity purification of GFP-tagged proteins — GFP-tagged factors representative of 90S and pre-60S r-particles were purified following a one-step GFP-Trap®_A procedure (Chromotek) as described in (90) with slight modifications. Briefly, GFP-tagged or untagged negative control cells harbouring the YCplac33-HA-RPL40A plasmid were grown in 200 ml of YPD medium to an OD_{600} of 0.8. Cells were washed with cold water, harvested and concentrated in 500 µl of ice-cold GFP lysis buffer (20 mM Tris-HCl, pH 7.5; 5 mM $MgCl_2$; 150 mM CH_3COOK; 1 mM DTT; 0.2% Triton X-100) containing a protease inhibitor cocktail (Complete, Roche). Cells were disrupted by vigorous shaking with glass beads in a Fastprep®-24 (MP Biomedicals) at 4 ºC and total extracts were clarified by centrifugation in a microfuge at the maximum speed (*ca*. 16,100 x *g*) for 10 min at 4 ºC. To each of the resulting supernatants, 25 µl of GFP-Trap®_A beads, equilibrated with the same buffer, were added and the mixture was incubated for 2 h at 4 ºC with end-over-end tube rotation. After incubation, the beads were washed six times with 1 ml the GFP lysis buffer at 4 ºC and resuspended in 100 µl of Laemmli buffer. Proteins were extracted by boiling for 10 min, separated in NuPAGE® SDS 4-12% gradient polyacrylamide gels (Invitrogen) and visualised by silver staining or western blotting. To normalise the amount of purified complexes to be loaded for comparative studies, aliquots of the samples were first resolved in the same conditions and visualised by silver staining according to manufacturer's instructions (Bio-Rad).

Fluorescence microscopy — To test pre-ribosomal particle export, the appropriate strains were transformed with the pRS314-RFP-NOP1-RPL25-eGFP or the pRS314-RFP-NOP1-RPS3-eGFP plasmid (gifts from J. Bassler) (91), which harbours the reporters Nop1-mRFP and L25-eGFP or Nop1-mRFP and S3-eGFP, respectively (**Table S3**). Transformants were grown in SGal-Trp medium and shifted to SD-Trp for 9 h to deplete L40. Cells were washed, resuspended in PBS buffer (140 mM NaCl, 8 mM Na_2HPO_4, 1.5 mM KH_2PO_4, 2.75 mM KCl, pH 7.3) and examined with a Leica DMR fluorescence microscope equipped with a DC350F digital camera and its software. Images were processed with Adobe® Photoshop® CS2 (Adobe Systems Incorporated).

To monitor whether L40 assembles in the nucleus, the JDY925 strain expressing an HA-tagged L40A from plasmid YCplac111-UBI-HA-RPL40A was transformed with plasmids pRS316-GAL-NMD3Δ100 (a gift from A. Jacobson) (92) and pRS314-RFP-NOP1-RPL25-eGFP (91). To monitor the localisation of HA-tagged L40A, we performed immunofluorescence with cells grown in SD-Leu-Ura-Trp or shifted for 24 h to SGal-Leu-Ura-Trp in order to induce the expression of the dominant negative Nmd3Δ100 protein. Immunofluorescence was performed as described previously (93). Primary monoclonal mouse anti-HA antibodies (HA.11, Covance) at a dilution of 1:500 and secondary goat anti-mouse Cy3-coupled antibody (Jackson Immunoresearch Laboratories) at 1:2000 were used to detect HA-L40A. DAPI (4',6-diamidino-2-phenylindole, Fluka) was used to stain DNA in the nucleus. Fluorescently labelled cells were inspected and processed as described above. Cells from the same cultures were also inspected for the GFP and RFP signal.

To study the subcellular location of Mex67, Mrt4, Nmd3, Rlp24, and Tif6 in the *GAL::RPL40* strain, plasmids pRS316-MEX67-GFP (a gift from J. Bassler) (94), YCplac33-MRT4-eGFP (61), pAJ755 (a gift from A. W. Johnson) (95), YCplac33-RLP24-eGFP, and pTIF6-GFP (a gift from A.J. Warren) (96) were used (see **Table S3**). To determine the subcellular location of Arx1, strain JDY910, which harbours a genomically GFP-tagged Arx1 (see **Table S1**) was transformed with pAS24-RPL40A and the resident YCplac33-UB-HA-RPL40A was counterselected on 5-fluoroorotic acid containing plates. Cells were grown in SGal-Leu-Ura or subjected to *in vivo* depletion in SD-Leu-Ura for different times. When required, DAPI (1 µg/ml final concentration) was added to the cultures during the last 3 h of growth. Fluorescently labelled cells were inspected and processed as described above.

Antibiotic sensitivity assays — The sensitivity to different drugs impairing translation was tested as follows; the wild-type strain, the *rpl40a* or *rpl40b* null mutants and the strain expressing the HA-tagged L40A protein were grown in YPD medium to an OD_{600} of 0.8 and diluted to an OD_{600} of 0.05. A series of ten-fold dilutions was done for each strain and 5 µl drops were spotted on YPD plates containing the indicated antibiotics at the specified range of concentrations: Anisomycin (from 5 to 15 µg/ml), Cycloheximide (from 0.025 to 0.1 µg/ml), Hygromycin B (from 5 to 20 µg/ml),

Paramomycin (from 0.1 to 2.5 mg/ml) and Neomycin (from 0.5 to 5 mg/ml). Plates were incubated at 30 ºC for 3-4 days.

The sordarin sensitivity assay was carried out in 96-well plates; the above strains were grown in YPD medium to an OD_{600} of 0.8 and diluted to an OD_{600} of 0.05 in 200 µl of YPD. Ten serial dilutions of the sordarin derivative GM193663 (Glaxo-Smith-Kline Research Center, Madrid; a gift from J.P.G. Ballesta) was done starting with the concentration of 4 µg/ml in the first well. The plates were incubated at 30 ºC with shaking and the OD_{600} was measured regularly at intervals of 2 h during 24-48 h. Inhibition was measured as the percentage of growth in wells containing *versus* controls lacking sordarin.

Preparation of ribosomes — Ribosomes were enriched as previously described (79). Briefly, 200 ml of cells expressing the HA-tagged or the untagged L40A r-protein were grown in YPD to an OD_{600} of 0.8, washed and concentrated in 500 µl of ice-cold buffer 1 [10 mM Tris-HCl, pH 7.4; 20 mM KCl; 12.5 mM $MgCl_2$; 5 mM 2-mercaptoethanol] containing a protease inhibitor cocktail (Complete EDTA-free, Roche). Cells were disrupted by vigorous shaking with glass beads in a Fastprep®-24 homogenizer (MP Biomedicals) at 4 ºC. A S30 fraction was obtained by centrifuging the extract at 16,100 x *g* for 20 min at 4 ºC in an Eppendorf microfuge. A crude ribosome pellet was prepared from the S30 fraction by centrifugation in a Beckman-Coulter Optima™ Max using a TL110 rotor at 90,000 r.p.m. for 60 min at 4 ºC. The pellet was resuspended in buffer 2 [20 mM Tris-HCl, pH 7.4; 100 mM $MgCl_2$; 5 mM 2-mercaptoethanol] and washed by centrifugation in a 20-40% discontinuous sucrose gradient in buffer 2 containing 500 mM ammonium acetate at 90,000 r.p.m. for 120 min at 4 ºC again in a TLA110 rotor. The pellet of washed ribosomes was dissolved in buffer 1 and stored at -80 ºC. Ribosomal proteins were separated in NuPAGE-SDS 4-12% gradient polyacrylamide gels (Invitrogen) and visualized by coomassie or western blotting with selected antibodies of the above described.

RESULTS

Generation of strains for the phenotypic analysis of the L40 protein — Yeast L40 is an essential r-protein of 52 amino acids with a predicted mass of 6.0 kDa and a basic pI of 11.05. As most yeast r-protein genes (97), L40 is encoded by two independent paralogous genes, *UBI1* (*RPL40A, YIL148W*) and *UBI2* (*RPL40B, YKR094C*). Their coding regions result in identical hybrid proteins that are specifically cleaved to yield ubiquitin and the r-protein L40 (98).

Early studies indicated that both *UBI1* and *UBI2* genes (hereafter *RPL40A* and *RPL40B* genes) are required for growth and normal accumulation of 60S r-subunits (66). The impact of a 4 h depletion of L40 on 60S r-subunit formation has been previously described in a systematic analysis of conditional mutants for expression of 26 distinct yeast essential 60S r-proteins (47). To characterise in detail the contribution of L40 to ribosome biogenesis, we first studied the phenotypic consequences of the deletion of either the *RPL40A* or the *RPL40B* gene. As shown in **Fig. 1*A***, the deletion of either *RPL40A* or *RPL40B* results in a mild growth defect, the one of *RPL40A* being slightly stronger. This result is in agreement with other reports (66,99) and is consistent with genome-wide expression data that suggest that *RPL40A* might contribute to 58% while *RPL40B* to 42% of total mRNA levels (100). To address the contribution of each L40 protein to 60S r-subunit production, we performed polysome profile analysis. As shown in **Fig. 1*B***, both the *rpl40a*Δ and *rpl40b*Δ *null* strains showed a mild deficit in 60S r-subunits with the *rpl40a*Δ strain being more affected than the *rpl40b*Δ strain. Quantification of total r-subunits by sucrose gradients indicated about a 5% reduction in the overall quantity of 60S r-subunits relative to the wild-type strain in both *rpl40a*Δ and *rpl40b*Δ strains (**data not shown**). Recent studies have suggested that duplicated paralogous r-proteins could play specific non-redundant roles in ribosome biogenesis and assembly (101). However, few extra copies of *RPL40A* or *RPL40B*, which were provided from centromeric plasmids, fully restored a wild-type growth rate and polysome profiles to the *rpl40b*Δ and *rpl40a*Δ strains, respectively (**Figs. S3** and **S4**). This suggests that there is no functional distinction between the L40A and L40B proteins at least under the laboratory conditions tested.

Depletion of L40 leads to a minor 60S ribosomal subunit shortage and a subunit joining defect — To further examine the function of L40, we constructed a *GAL::RPL40A rpl40b*Δ strain (hereafter named the *GAL::RPL40* strain; see "Experimental Procedures" and **Table S1**). Growth of this strain was not different from that of the isogenic wild type strain on permissive YPGal medium but was progressively slowed after shifting to repressive YPD medium and ceased after approximately 12 h (**Fig. 2*A***). To address the contribution of L40 to 60S r-subunit production, we first performed polysome profile

analysis. As shown in **Fig. 2*B***, and complementing previous data (47), the *GAL::RPL40* strain displayed practically normal polysome profiles when grown in YPGal. When shifted for 12 h to YPD, it showed a clear decrease in polysomes and the appearance of half-mer polysomes. These features were even more pronounced upon a 24 h shift to YPD (**Fig. 2*B***). Wild-type cells showed no alterations in the polysome profile when transferred to YPD (**data not shown**). Intriguingly, there was almost no decrease in the free 60S/40S ratio for the L40-depleted strain after the shift to YPD (**Fig. 2*B***). This could be due to the accumulation of arrested pre-60S r-particles, to a simultaneous deficit of both r-subunits and/or, most likely, to a 60S r-subunit joining defect in translation initiation upon depletion of L40 (see "Discussion"). Consistently, quantification of total r-subunits by run-off and low-Mg^{2+} sucrose gradients showed that depletion of L40 leads to only 10% reduction of the 60S to 40S r-subunit ratio compared to the wild-type control upon 12 h of depletion (**data not shown**). We therefore conclude that depletion of L40 leads to a minor deficit in 60S relative to 40S r-subunits and a 60S r-subunit joining defect.

Depletion of L40 slightly delays rRNA processing at ITS2 — To determine whether depletion of L40 impairs ribosome biogenesis, we assessed the kinetics of rRNA accumulation by pulse-chase labelling experiments in wild-type and *GAL::RPL40* cells shifted for 12 h to SD-Ura medium (see "Experimental procedures"). Cells were pulse-labelled for 2 min with [5,6-^{3}H]-uracil, then chase for 5, 15, 30 and 60 min with a large excess of non-radioactive uracil. Compared to the wild-type cells, the *GAL::RPL40* cells showed delayed processing of 35S pre-rRNA as shown by the abundance and persistence of this precursor in early chase time points. This was combined with some loss of $27SA_2$ and 20S pre-rRNA and the appearance of the aberrant 23S pre-rRNA species (**Fig. 3*A***). More importantly, some 27SB pre-rRNAs persisted until the last time-point of the chase. However, a gradual decrease in 27SB pre-rRNAs is observed over the chase, thus suggesting efficient turnover of these precursors. A minor accumulation of 7S pre-rRNAs is also perceived (**Fig. 3*B***). Interestingly, the production of mature rRNAs is minimally affected (**Fig. 3**). Thus, the minor 60S r-subunit shortage detected in the L40-depleted cells is likely the consequence of the slight delay in 27SB and 7S pre-rRNA processing detected in these cells. We conclude that 60S r-subunit biogenesis could continue at almost the wild-type rate in the absence of the L40 r-protein.

To assess whether L40 has a role in pre-rRNA processing, we analysed the steady-state levels of pre- and mature rRNAs by northern hybridisation during a time-course of L40 depletion. Consistent with the pulse-chase data, a certain decrease in the levels of mature rRNAs was observed after depletion of L40 especially at later time points (**Fig. 4**). The 35S and the aberrant 23S pre-rRNAs accumulated with ongoing depletion (**Fig. 4*A***). These accumulations are consistent with delayed pre-rRNA processing at early cleavage sites. Probably, in part as a consequence of this delay, the levels of the 20S pre-rRNA but more significantly those of the $27SA_2$ pre-rRNA decreased (**Fig. 4*A***). Finally, we detected almost no changes in levels of 27SB pre-rRNAs (**Fig. 4*A***) and a modest accumulation of 7S pre-rRNAs (**Fig. 4*B***).

To increase the resolution of the pre-rRNA analysis, we also performed primer extension analyses upon depletion of L40 (**Fig. 4*C***). The levels of $27SA_2$ and $27SA_3$ pre-rRNAs were clearly lower, as shown by the primer extension stop at site A_2 and A_3, respectively. In contrast, the levels of $27SB_L$ and $27SB_S$ modestly increased, as shown by the primer extension stops at B_{1L} and B_{1S}, respectively. Finally, primer extension analysis through site C_2 displayed a clear increase in the level of the 25.5S pre-rRNA upon depletion of L40.

Altogether, our results indicate that L40 is not essential for the maturation of rRNAs. Instead, L40 seems to be needed to optimise the pre-rRNA processing reactions occurring within the ITS2 region. Hence, the cleavage at site C_2 and especially the further exonucleolytic trimming of 7S and 25.5S pre-rRNAs to mature 5.8S and 25S rRNAs, respectively, are slightly delayed upon L40 depletion.

Depletion of L40 impairs export of pre-60S r-particles from the nucleus to the cytoplasm — To determine whether L40 depletion impairs nuclear export of pre-60S r-particles, we analysed the location of the L25-eGFP 60S reporter (91) in the *GAL::RPL40* strain. Under permissive culture conditions (SGal-Ura) or after short shifts to non-permissive conditions (3-6 h in SD-Ura), L25-eGFP was found predominantly in the cytoplasm in the *GAL::RPL40* strain (**Fig. 5** and **data not shown**). However, following a longer shift to glucose-containing medium (9-12 h in SD-Ura), *GAL:RPL40* cells exhibited an accumulation of the L25-eGFP fluorescence signal all over the nucleus without evident

restriction to the nucleolus (**Fig. 5**). Similar results were obtained when the L11B-eGFP 60S reporter was used (102) (**data not shown**). These observations are specific for the large r-subunit since the location of the S2-eGFP and S3-eGFP 40S r-subunit reporters was cytoplasmic in either SGal-Ura medium or upon a long shift to SD-Ura medium (**Fig. 5** and **data not shown**). The wild-type strain was also examined; no nuclear fluorescence accumulation for any of the above r-reporters was observed either in SGal-Ura or in SD-Ura medium (**data not shown**). We conclude that pre-60S r-particles are retained in the nucle(ol)us at later time points of L40 depletion.

L40 assembles in the cytoplasm — Assembly of r-subunits occurs mainly in the nucle(ol)us, although few 60S r-proteins appear to be loaded exclusively, such as L24 (49,58) or preferentially, such as L10 or P0 (56,61,103,104) onto cytoplasmic pre-60S r-particles. Pulse-chase studies performed in the 70's suggest that yeast L40 associates at a late stage of the 60S r-subunit assembly process (49). The presence of a nuclear localisation sequence (NLS) within L40 (cNLS mapper programme, (105)) suggests that L40 assembly may occur in the nucleus. To study precisely in which cellular compartment L40 assembles, we made use of an *rpl40* null strain expressing HA-tagged L40A from a centromeric plasmid (see "Experimental procedures" and **Table S1**). The resulting strain displayed almost wild-type growth and polysome profiles (**Figs. S5*A*-*B***). Moreover, the HA-L40A protein assembles efficiently into ribosomes (**Fig. S5*C***).

Since export of pre-60S r-particles is largely dependent on the exportin Crm1/Xpo1, which is one of several pre-60S export factors identified in yeast (106-111), and its pre-60S adaptor protein Nmd3 (106,112), we monitored the cytoplasmic or nuclear localisation of the HA-L40A protein upon overexpression of a wild-type Nmd3 protein or the dominant-negative, truncated Nmd3Δ100 protein. The mutant Nmd3Δ100 protein essentially lacks the C-terminally located nuclear export sequence (NES) signals that mediate nuclear export but retains the ability to bind to pre-60S r-particles, thus, it specifically traps these particles in the nucleus (92). Under non-inducible conditions or when the wild-type Nmd3 protein was overexpressed, HA-L40A was detected in the cytoplasm of all cells examined (**Fig. 6** and **data not shown**). Strikingly, no change in the cytoplasmic distribution of HA-L40A was found upon overexpression of the Nmd3Δ100 protein (**Fig. 6**). As a control, we used the L25-eGFP reporter, which was simultaneously co-expressed with HA-L40A in the *rpl40* null strain. L25-eGFP has been described to assemble in the nucle(ol)us (e.g., (60,106,113)). As expected, this reporter remained cytoplasmic in non-induced cells but was clearly found in the nucleus of cells expressing the Nmd3Δ100 protein (**Fig. 6**).

Altogether, these data suggest that, independently of the predicted presence of NLS sequences, L40 assembles predominantly at the level of cytoplasmic pre-60S r-particles.

L40 associates with very late/cytoplasmic pre-60S ribosomal particles — To investigate in more detail the timing of the assembly of L40 with pre-60S r-particles, we first immunoprecipitated HA-L40 containing complexes from whole cell extracts and assayed co-purified pre-rRNA species and r-proteins by northern hybridisation and western blotting, respectively. As shown in **Fig. 7**, there was a significant co-precipitation of L1 and L35 r-proteins (**Fig. 7*A***) and mature 5.8S and 5S rRNAs (**Fig. 7*B***) with the tagged HA-L40A protein, indicating that r-particles rather than soluble HA-L40 were immunoprecipitated. The precipitation was specific since neither r-proteins nor RNA were enriched from extracts of an untagged strain (**Fig. 7*A*-*B***). Interestingly, no 7S pre-rRNAs were detected, suggesting that either the HA tag is not accessible for immunoprecipitation when HA-L40 is present in nuclear pre-60S r-particles or the HA-L40 protein assembles into late pre-60S intermediates, which have completed the pre-rRNA processing reactions. To distinguish between these two possibilities, we screened for the presence of HA-L40 following purification of GFP-tagged proteins specific for 90S (Nop58/Nop5) (53,114), early, intermediate, late and cytoplasmic pre-60S r-particles (Ssf1, Nsa1, Nop7/Yph1, Arx1 and Kre35/Lsg1) (52,115-119) and mature 60S r-subunits (P0) (120) (see **Fig. S2**). Purified particles were analysed by SDS-PAGE, and HA-L40 was detected by western blotting using anti-HA antibodies. Antibodies against selected pre-ribosomal factors (Nop1, Has1 and Mrt4) and other 60S r-proteins (L1 and L3) were also used to define the pre-60S r-particles at the different stages of their maturation. This analysis revealed that HA-L40 was only significantly enriched in P0-eGFP containing particles, which mainly represent mature 60S r-subunits (**Fig. 8**). HA-L40 was practically absent from early (Ssf1-eGFP and Nop7-eGFP) and intermediate pre-60S particles

(Nsa1-eGFP) and very modestly represented in 90S (Nop58-eGFP) and late (Arx1-eGFP) and cytoplasmic (Arx1-eGFP and Kre35-eGFP) pre-60S particles (**Fig. 8**). In clear contrast, L1 and L3 were present, as previously reported (61,90,116), in all tested pre-ribosomal particles. Finally, and as expected, Nop1 is mainly associated with 90S pre-ribosomal particles (114), Has1 with 90S and early and intermediate pre-60S r-particles (90) and Mrt4 with intermediate and late/cytoplasmic pre-60S r-particles (61).

Altogether, these results reveal that L40 associates with late/cytoplasmic pre-60S r-particles but is only stably assembled into mature cytoplasmic 60S r-subunits.

L40 is required for the release of Nmd3 and Rlp24 from cytoplasmic pre-60S ribosomal particles — Recent reports on the complete structure of the eukaryotic large r-subunit have allowed the visualisation of the L40 protein within mature ribosomes (7,10). These structures reveal that L40 is positioned close to the binding site for the eukaryotic elongation factors (eEFs) in the intersubunit joining face of the mature 60S r-subunit (7,10) (see also **Fig. 9*A***). Hence, L40 binds to RNA residues in proximity to the GTPase-associated center (GAC) in domain II of 25S rRNA, the peptidyl-transferase center (PTC) in domain V and the sarcin-ricin loop (SRL) in domain VI of 25S rRNA (**Figs. 9*B*-*C***). Several other r-proteins are clear neighbours of L40 amongst them L9, L10, L12, L20 and the ribosomal P-protein stalk (**Fig. 9*A***). Interestingly, Sengupta *et al.* have mapped the binding site of Nmd3 in a region that might overlap with the binding sites of L40 and its closest neighbours (121,122). This site has been described to be close to the position of Tif6, which binds on the edge of the 60S r-subunit joining face (7,123). Thus, we found it particularly pertinent to examine whether assembly of L40 was a prerequisite for recycling of Nmd3 and/or Tif6. To assess this point, GFP-tagged versions of Nmd3, Tif6 and other nucleo-cytoplasmic shuttling factors, such as Arx1, Mex67, Mrt4, and Rlp24 were expressed in the *GAL::RPL40* strain and their localisation studied before or after L40 depletion. As previously reported (52,58,61,94,112,124), all these proteins, albeit to different extents, display both nuclear and cytoplasmic localisation under permissive conditions (**Figs. 10** and **S6**). Importantly, although no mislocalisation of Arx1-, Mex67-, Mrt4- and Tif6-GFP could be observed, Nmd3- and Rlp24-GFP were retained in the cytoplasm upon 18 h depletion of L40 (**Figs. 10** and **S6**). Since Nmd3 is equally distributed between cytoplasm and nucleoplasm at steady state, it is difficult to observe a clear-cut cytoplasmic redistribution of this protein (95,103,125,126); however and in agreement with its cytoplasmic retention, we observed nuclear exclusion of Nmd3-GFP upon L40 depletion (**Fig. 10** and **S6**). To distinguish between an impairment of the release of Nmd3 and Rlp24 from cytoplasmic pre-60S r-particles or a defect in recycling free Nmd3 and Rlp24 to the nucle(ol)us, we subjected extracts from the *GAL::RPL40* strain expressing GFP-tagged versions of each of these factors, before or after a 18 h shift to glucose containing medium, to sucrose gradient fractionation. Then, fractions were analysed by western blot using anti-GFP antibodies to detect GFP-tagged Nmd3 or Rlp24, respectively. As shown in **Fig. S7**, we could not detect significant changes in the pattern of sedimentation of Nmd3-GFP or Rlp24-GFP upon L40 depletion, which were still found in the 60S region of the gradients. This result indicates that these proteins remain bound to high-molecular-mass complexes, most likely aberrant cytoplasmic pre-60S r-particles, upon L40 depletion.

Taken together, our data indicate that Nmd3 and Rlp24 require L40 to be efficiently displaced from cytoplasmic pre-60S r-particles in order to recycle back to the nucle(ol)us.

Expression of HA-L40A leads to sordarin resistance while rpl40aΔ and rpl40bΔ cells show hyper-sensitivity to this compound — Both, the GAC and the SRL has been proposed to interact directly with the G domain of eEFs (see (36,127) and references therein). Moreover, the r-stalk (P-proteins and L12), which is in close proximity of L40 (**Fig. 9*A***), has also been previously identified to interact with eEF2 (36). Both eEF2 and r-stalk proteins have been described to be targets of members of the sordarin family of antifungal compounds (69,70,128,129). To evaluate whether L40 could mediate inhibition by or resistance to sordarin, we tested the capability of the single *rpl40aΔ* and *rpl40bΔ* strains or the *rpl40* null mutant expressing as the sole source of L40 a HA-tagged version of L40A to grow in liquid YPD medium containing increasing concentrations of the sordarin derivative GM193663. As a control, we used both an isogenic wild-type and *rpl35bΔ* strain. As shown in **Fig. 11**, we found that the strain expressing the HA-tagged L40A r-protein is highly resistant to sordarin resulting in a more than 30-fold increase in the 50% inhibitory concentration (IC_{50}) value compared to its

isogenic wild-type counterpart. In contrast, the single *rpl40aΔ* and specially the *rpl40bΔ* mutant were clearly much more sensitive to this drug than the wild-type strain; the IC_{50} value obtained for the *rpl40aΔ* and *rpl40bΔ* mutants were at least 10-fold lower than that of the wild-type strain. Interestingly, this sensitivity is not simply related to lower dosage of an r-protein since the IC_{50} value of an *rpl35bΔ* mutant is practically identical to that of the wild-type strain. Moreover, the effect of sordarin seems to be very specific since we could not observed enhanced sensitivity or resistance to other translation antibiotics (anisomycin, cycloheximide, hygromycin B, paromomycin and neomycin) for the above strains when compared to their isogenic wild-type counterpart. Finally, to test if the sordarin resistance of the strain expressing the HA-L40A protein is the indirect result of the destabilisation of r-proteins such as L12, L1 or P0, whose loss-of-function mutations have been reported to induce sordarin resistance (68,128), we prepared samples enriched in pre-ribosomal particles and mature ribosomes containing either wild-type L40 or HA-tagged L40A (see "Experimental Procedures") and washed them with a high salt solution (0.5 M NH_4Cl). As shown in **Fig. S8**, no differences were detected in the purification rate of a subset of r-proteins, including L12, L1 and P0. Thus, these r-proteins are stably associated with ribosomes both in wild-type and HA-L40A expressing strain.

Taken together, these results suggest that L40 specifically and functionally interacts with eEF2 during translation elongation.

DISCUSSION

In this work, we have addressed the role of yeast L40 r-protein in 60S r-subunit biogenesis and function. L40 was not modelled in the crystal structure of the 50S r-subunit from *Haloarcula marismortui* (11) and it has only been recently localised in the structure of eukaryotic 60S r-subunits from *S. cerevisiae* or *Tetrahymena thermophila* (7,10) (see **Fig. 9**).

Two strain systems were used for the phenotypical analysis of L40 r-protein. First, we analysed single *rpl40a* and *rpl40b* null mutants. Our results indicate that both genes contribute to growth and normal accumulation of 60S r-subunits, with the role of *RPL40A* being apparently more important than that of *RPL40B* (**Fig. 1**). While a functional specificity between many paralogous r-proteins has been described (101,130,131), we could not find any distinction between L40A and L40B at least for growth and polysome profile analyses under standard laboratory conditions (**Fig. S3-4**). Second, we established a conditional *rpl40* null strain by disrupting the *RPL40B* gene and placing the ORF of *RPL40A* under the control of a *GAL* promoter, which allows genetic depletion of the L40 r-protein by transcriptional repression in cells growing with glucose as carbon source. Polysome profile analyses strongly indicate that 60S r-subunits lacking L40 are defective in subunit joining (see below) and suggest that both r-subunits may have an increased susceptibility to degradation at longer time points of L40 depletion (**Fig. 2**); similar observations were made for the null *rpl24* mutant and upon L1 depletion (47,132,133).

Consistent with the polysome profile results, pulse-chase labelling, northern hybridisation and primer extension analyses in the L40-depleted strain indicate that L40 is practically dispensable for pre-rRNA processing. Thus, we could only observe a modest delay in 27SB and 7S pre-rRNA processing upon depletion of L40 (**Fig. 3**). Consequently, the relative amounts of these precursors slightly increase although the steady-state levels of mature 25S and 5.8S rRNA only decrease at late time points of depletion (**Fig. 4**). In addition, the depletion of L40 leads to a mild delay in early cleavage events of pre-rRNA processing at the A_0, A_1 and A_2 sites that have subsequent consequences for the levels of 20S pre-rRNA and mature 18S (**Figs. 3** and **4**); this delay has been extensively reported for many mutants in genes encoding 60S r-subunit assembly factors and 60S r-proteins and is likely due to inefficient recycling of *trans*-acting factors that cannot efficiently dissociate from aberrant pre-60S r-particles (for further discussion, see (23,134)). These data strongly suggest that L40 is not strictly required for the pre-rRNA processing reactions and that ribosomes lacking L40 are efficiently degraded. This is very unusual since all essential 60S r-proteins studied so far, except perhaps L1 (47,133) and L10 (82), play critical roles during ribosome maturation. Strikingly, pre-60S particles are retained in the nucle(ol)us upon depletion of L40 (**Fig. 5**). Therefore, we must assume that, although pre-rRNA processing reactions are apparently taking place in a correct way, pre-60S particles from L40-depleted cells are not fully competent for nucleo-cytoplasmic export. We have shown that a HA-tagged L40 is predominantly assembled in the cytoplasm (see below), thus, we are tempted to speculate that wild-type nuclear pre-60S r-particles are devoid of L40 and most likely retention of these

particles upon L40 depletion, as well as the abovementioned 23S pre-rRNA accumulation, is occurring as a secondary effect due to inefficient recycling of a critical nucleo-cytoplasmic shuttling factor to the nucleus. A scenario similar to this one has already been demonstrated for the nuclear shuttling factors Nmd3, Mrt4 and Rlp24, which are recycled to the nucleus upon cytoplasmic assembly of L10 (56), P0 (61,104,135) and L24 (136), respectively (for further discussion see (20,103,126)). Interestingly, our data demonstrate that L40 is an additional r-protein involved in the release of Nmd3 and Rlp24 from cytoplasmic pre-60S r-particles (**Figs. 10, S6** and **S7**). How does the depletion of L40 block the release of these factors? One possibility is that L40 acts as an effector of the energy-consuming factors involved in the release of Nmd3 and Rlp24 from cytoplasmic pre-60S r-particles. So far, the GTPase Kre35 (95) and the AAA-ATPase Drg1 (137) are the factors described to be required for the release of Nmd3 and Rlp24, respectively. Drg1, which is apparently one of the earliest acting factors acting during the cytoplasmic maturation of 60S r-subunits, is required for the release of other factors in addition to Rlp24, among them Arx1, Mrt4, Nog1, and Tif6 (103,126,137); however, our results show that the recycling of Arx1 and Tif6 seems not to be affected by the depletion of L40 (**Fig. 10**). Kre35 is apparently one of the latest acting factors in this process (95,103) and the release of Nmd3 by Kre35 also requires the r-protein L10. Thus, another possibility that could explain the lack of proper release of these factors upon L40 depletion is that assembly of L40 is coordinated to that of L10; indeed, although the structural analyses suggest that Nmd3 and L10 can bind simultaneously to pre-60S r-particles (7,10,122), co-immunoprecipitation data are fully consistent with a model in which L10 could be preferentially loaded after Nmd3 release onto cytoplasmic pre-60S particles in wild-type conditions (56). Interestingly, analyses of the 60S r-subunit structure suggest that Nmd3 and L40 must sequentially associate with pre-60S particles since their binding sites on 60S r-subunits seem mutually exclusive (7,10,122). More puzzling is the role of L40 in the release of Rlp24 from cytoplasmic pre-60S r-particles. It has been hypothesized that Rlp24 and L24 successively occupy the same rRNA binding site during ribosome synthesis (58). If this hypothesis is correct, the binding site of Rlp24 would be placed about 10 nm away from that of L40 and therefore, a wave of conformational changes is required to explain our observation. Surprisingly, whether L10 is required to release Rlp24 from pre-60S r-particles has so far not been addressed. Clearly, understanding the precise mechanism by which L40 participates in the recycling of Nmd3 and Rlp4 will require further work.

We have also addressed the course of assembly of L40. Previous data suggested that yeast L40 might associate with pre-60S particles at a relatively late stage during the course of 60S r-subunit assembly (49). Here, we present several lines of evidence that yeast L40 may assemble in the cytoplasm, in complete agreement with the above described role in the release of shuttling factors (**Figs. 6**, **7**, **8** and **S2**). However, we cannot fully exclude the possibility, as also suggested by the presence of predicted NLS sequences within L40, that some assembly could take place in the nucleus in wild-type conditions and that the HA tag could partially interfere with the import of the HA-L40 protein. Besides L40, few other r-proteins have been described to assemble exclusively (L24 and L10) or predominantly (P0) in the cytoplasm (56,58,61,103,104,135,136). Further experiments are required to discard the possibility that L40 may also assemble into pre-60S particles within the nucleus.

Finally, we have addressed the function of L40 in translation. As stated by Wilson and Nierhaus (138), the assignment of a specific role, in terms of translational activity, to an individual given r-protein is extremely difficult. This is based on the highly cooperative nature of the interactions between rRNA and r-proteins and between the r-proteins themselves. Indeed, there are many reports describing that even small changes in the primary sequence of an r-protein have significant, long distance effects on the rRNA structure (e.g. (30,59,139-141)). Our data suggest that L40 is required for the joining of 60S and 40S r-subunits and for the translocation process during translation. Both functions are fully consistent with the position of L40 on the mature 60S r-subunit (7,10). The r-subunit joining role of L40 is inferred from the analysis of the polysome profiles of *rpl40aΔ* and *rpl40bΔ* mutants but especially of those of L40-depleted cells. These polysome profiles showed a pronounced decrease in 80S and polysomes and, more importantly, the accumulation half-mer polysomes without a net reduction in the levels of free 60S r-subunits, as indicated by a ratio of free 60S to 40S r-subunits that is relatively similar to that of wild-type cells (**Fig. 2**). Interestingly, the L10 and L11 r-proteins, which

are close neighbours of L40 (7,10) (**Fig. 9*A***), have been previously involved in r-subunit joining (82,142). Moreover, a mutational change in the L33 r-protein, identified due to its Gcd$^-$ phenotype (derepression of Gcn4 translation), has been suggested to impede the r-subunit joining reaction (143). Consistent with this finding, our preliminary data suggest that both the *rpl40aΔ* strain and, to the lesser extent, the *rpl40bΔ* mutant confer a Gcd$^-$ phenotype that could be suppressed by overexpression of the translation initiation ternary complex components eIF2 and $tRNA_i^{Met}$ (A. Fernández-Pevida and J. de la Cruz, unpublished results). Due to the fact that Nmd3 is locked on cytoplasmic pre-60S particles upon L40 depletion (see above), further experiments are needed to determine whether L40 has a direct role in the r-subunit joining reaction since the location of Nmd3 within pre-60S r-particles is apparently incompatible with the joining of 60S and 40S r-subunits (122). In agreement with this, it has been shown that Nmd3 does not bind to 80S ribosomes or polysomes (144). In addition, we hypothesise that L40 participates in the translocation process during translation. This is deduced from the selective sordarin hypersensitivity of the *rpl40aΔ* and *rpl40bΔ* mutants and the increased resistance to this drug of cells expressing HA-tagged L40 as the sole source of L40 (**Fig. 11**). Sordarin derivatives inhibit fungal protein synthesis by stabilising the eEF2-ribosome complex (69,70), and many sordarin-resistant mutations, which allow eEF2 to function in translocation even when bound to a sordarin molecule, are linked to the genes that encode eEF2 and the r-stalk P0 and L12 proteins (68-70,128,129,145). Thus, these observations support a role for the r-stalk proteins during translation elongation. Our observations that L40 is another target of sordarin strongly suggest that eEF2 and L40 may also interact functionally during the conformational switch that occurs during translation elongation. Whether L40 makes physical contact with eEF2 or whether the HA-L40 protein exerts sordarin resistance by affecting the functionality of r-stalk proteins or cytoplasmic assembly factors, e.g. the eEF2-related GTPase Efl1/Ria1 (124,126,146), remains to be elucidated.

In conclusion, we have shown that L40 assembles late into pre-60S subunits and may participate in r-subunit joining and eEF2 function during the translation process. Future in-depth analyses will be required to understand the mechanistic details of the role of L40 during cytoplasmic 60S r-subunit assembly as well as during the initiation and elongation steps of translation.

REFERENCES

1. Schmeing, T. M., and Ramakrishnan, V. (2009) What recent ribosome structures have revealed about the mechanism of translation. *Nature* **461**, 1234-1242
2. Spahn, C. M., Beckmann, R., Eswar, N., Penczek, P. A., Sali, A., Blobel, G., and Frank, J. (2001) Structure of the 80S ribosome from *Saccharomyces cerevisiae*-tRNA-ribosome and subunit-subunit interactions. *Cell* **107**, 373-386
3. Chandramouli, P., Topf, M., Menetret, J. F., Eswar, N., Cannone, J. J., Gutell, R. R., Sali, A., and Akey, C. W. (2008) Structure of the mammalian 80S ribosome at 8.7 Å resolution. *Structure* **16**, 535-548
4. Taylor, D. J., Devkota, B., Huang, A. D., Topf, M., Narayanan, E., Sali, A., Harvey, S. C., and Frank, J. (2009) Comprehensive molecular structure of the eukaryotic ribosome. *Structure* **17**, 1591-1604
5. Armache, J. P., Jarasch, A., Anger, A. M., Villa, E., Becker, T., Bhushan, S., Jossinet, F., Habeck, M., Dindar, G., Franckenberg, S., Marquez, V., Mielke, T., Thomm, M., Berninghausen, O., Beatrix, B., Soding, J., Westhof, E., Wilson, D. N., and Beckmann, R. (2010) Localization of eukaryote-specific ribosomal proteins in a 5.5-A cryo-EM map of the 80S eukaryotic ribosome. *Proc Natl Acad Sci USA* **107**, 19754-19759
6. Armache, J. P., Jarasch, A., Anger, A. M., Villa, E., Becker, T., Bhushan, S., Jossinet, F., Habeck, M., Dindar, G., Franckenberg, S., Marquez, V., Mielke, T., Thomm, M., Berninghausen, O., Beatrix, B., Soding, J., Westhof, E., Wilson, D. N., and Beckmann, R. (2010) Cryo-EM structure and rRNA model of a translating eukaryotic 80S ribosome at 5.5-A resolution. *Proc Natl Acad Sci USA* **107**, 19748-19753
7. Klinge, S., Voigts-Hoffmann, F., Leibundgut, M., Arpagaus, S., and Ban, N. (2011) Crystal Structure of the Eukaryotic 60S Ribosomal Subunit in Complex with Initiation Factor 6. *Science*

8. Rabl, J., Leibundgut, M., Ataide, S. F., Haag, A., and Ban, N. (2011) Crystal structure of the eukaryotic 40S ribosomal subunit in complex with initiation factor 1. *Science* **331**, 730-736
9. Ben-Shem, A., Jenner, L., Yusupova, G., and Yusupov, M. (2010) Crystal structure of the eukaryotic ribosome. *Science* **330**, 1203-1209
10. Ben-Shem, A., Garreau de Loubresse, N., Melnikov, S., Jenner, L., Yusupova, G., and Yusupov, M. (2011) The structure of the eukaryotic ribosome at 3.0 Å resolution. *Science* **334**, 1524-1529
11. Ban, N., Nissen, P., Hansen, J., Moore, P. B., and Steitz, T. A. (2000) The complete atomic structure of the large ribosomal subunit at 2.4 Å resolution. *Science* **289**, 905-920
12. Wimberly, B. T., Brodersen, D. E., Clemons, W. M., Morgan-Warren, R. J., Carter, A. P., Vonrhein, C., Hartsch, T., and Ramakrishnan, V. (2000) Structure of the 30S ribosomal subunit. *Nature* **407**, 327-339
13. Schluenzen, F., Tocilj, A., Zarivach, R., Harms, J., Bashan, A., Bartels, H., Agmon, I., Franceschi, F., and Yonath, A. (2000) Structure of functional activated small ribosomal subunit at 3.3 Å resolution. *Cell* **102**, 615-623
14. Selmer, M., Dunham, C. M., Murphy, F. V. t., Weixlbaumer, A., Petry, S., Kelley, A. C., Weir, J. R., and Ramakrishnan, V. (2006) Structure of the 70S ribosome complexed with mRNA and tRNA. *Science* **313**, 1935-1942
15. Verschoor, A., Warner, J. R., Srivastava, S., Grassucci, R. A., and Frank, J. (1998) Three-dimensional structure of the yeast ribosome. *Nucleic Acids Res* **26**, 655-661
16. Wool, I. G. (1979) The structure and function of eukaryotic ribosomes. *Annu Rev Biochem* **48**, 719-754
17. Henras, A. K., Soudet, J., Gerus, M., Lebaron, S., Caizergues-Ferrer, M., Mougin, A., and Henry, Y. (2008) The post-transcriptional steps of eukaryotic ribosome biogenesis. *Cell Mol Life Sci* **65**, 2334-2359
18. Fromont-Racine, M., Senger, B., Saveanu, C., and Fasiolo, F. (2003) Ribosome assembly in eukaryotes. *Gene* **313**, 17-42
19. Mélèse, T., and Xue, Z. (1995) The nucleolus: an organelle formed by the act of building a ribosome. *Curr Opin Cell Biol* **7**, 319-324
20. Panse, V. G., and Johnson, A. W. (2010) Maturation of eukaryotic ribosomes: acquisition of functionality. *Trends Biochem Sci* **35**, 260-266
21. Gerbi, S. A., and Borovjagin, A. V. (2004) Pre-ribosomal RNA processing in multicellular organisms. in *Nucleolus* (Olson, M. O. J. ed.), Landes Biosciences/Eurekah.com, Georgetown. pp 170-198
22. Eichler, D. C., and Craig, N. (1994) Processing of eukaryotic ribosomal RNA. *Prog Nucleic Acid Res Mol Biol* **49**, 197-239
23. Venema, J., and Tollervey, D. (1999) Ribosome synthesis in *Saccharomyces cerevisiae*. *Annu Rev Genet* **33**, 261-311
24. Nomura, M., Nogi, Y., and Oakes, M. (2004) Transcription of rDNA in the yeast *Saccharomyces cerevisiae*. in *Nucleolus* (Olson, M. O. J. ed.), Landes Bioscience/Eurekah.com, Georgetown. pp 128-153
25. Strunk, B. S., and Karbstein, K. (2009) Powering through ribosome assembly. *RNA* **15**, 2083-2104
26. Kressler, D., Hurt, E., and Bassler, J. (2010) Driving ribosome assembly. *Biochim Biophys Acta* **1803**, 673-683
27. Dinman, J. D. (2009) The eukaryotic ribosome: current status and challenges. *J Biol Chem* **284**, 11761-11765
28. Dresios, J., Panopoulos, P., Suzuki, K., and Synetos, D. (2003) A dispensable yeast ribosomal protein optimizes peptidyltransferase activity and affects translocation. *J Biol Chem* **278**, 3314-3322
29. Dresios, J., Derkatch, I. L., Liebman, S. W., and Synetos, D. (2000) Yeast ribosomal protein L24 affects the kinetics of protein synthesis and ribosomal protein L39 improves translational accuracy, while mutants lacking both remain viable. *Biochemistry* **39**, 7236-7244
30. Petrov, A., Meskauskas, A., and Dinman, J. D. (2004) Ribosomal protein L3: influence on ribosome structure and function. *RNA Biol* **1**, 59-65
31. Meskauskas, A., and Dinman, J. D. (2007) Ribosomal protein L3: gatekeeper to the A site. *Mol Cell* **25**, 877-888

32. Meskauskas, A., and Dinman, J. D. (2001) Ribosomal protein L5 helps anchor peptidyl-tRNA to the P-site in *Saccharomyces cerevisiae*. *RNA* **7**, 1084-1096
33. Kramer, G., Boehringer, D., Ban, N., and Bukau, B. (2009) The ribosome as a platform for co-translational processing, folding and targeting of newly synthesized proteins. *Nature Struct Mol Biol* **16**, 589-597
34. Valasek, L., Mathew, A. A., Shin, B. S., Nielsen, K. H., Szamecz, B., and Hinnebusch, A. G. (2003) The yeast eIF3 subunits TIF32/a, NIP1/c, and eIF5 make critical connections with the 40S ribosome in vivo. *Genes Dev* **17**, 786-799
35. Dalley, J. A., Selkirk, A., and Pool, M. R. (2008) Access to ribosomal protein Rpl25p by the signal recognition particle is required for efficient cotranslational translocation. *Mol Biol Cell* **19**, 2876-2884
36. Gómez-Lorenzo, M. G., Spahn, C. M., Agrawal, R. K., Grassucci, R. A., Penczek, P., Chakraburtty, K., Ballesta, J. P. G., Lavandera, J. L., García-Bustos, J. F., and Frank, J. (2000) Three-dimensional cryo-electron microscopy localization of EF2 in the *Saccharomyces cerevisiae* 80S ribosome at 17.5 A resolution. *EMBO J* **19**, 2710-2718
37. Briones, E., Briones, C., Remacha, M., and Ballesta, J. P. G. (1998) The GTPase center protein L12 is required for correct ribosomal stalk assembly but not for *Saccharomyces cerevisiae* viability. *J Biol Chem* **273**, 31956-31961
38. Gingras, A. C., Raught, B., and Sonenberg, N. (2004) mTOR signaling to translation. *Curr Top Microbiol Immunol* **279**, 169-197
39. Ballesta, J. P. G., Rodriguez-Gabriel, M. A., Bou, G., Briones, E., Zambrano, R., and Remacha, M. (1999) Phosphorylation of the yeast ribosomal stalk. Functional affects and enzymes involved in the process. *FEMS Microbiol Rev* **23**, 537-550
40. McCoy, L. S., Xie, Y., and Tor, Y. (2011) Antibiotics that target protein synthesis. *Wiley Interdiscip Rev RNA* **2**, 209-232
41. Yonath, A. (2005) Antibiotics targeting ribosomes: resistance, selectivity, synergism and cellular regulation. *Annu Rev Biochem* **74**, 649-679
42. Vilardell, J., and Warner, J. R. (1997) Ribosomal protein L32 of *Saccharomyces cerevisiae* influences both the splicing of its own transcript and the processing of rRNA. *Mol Cell Biol* **17**, 1959-1965
43. Fewel, S. W., and Woolford, J. L., Jr. (1999) Ribosomal protein S14 of *Saccharomyces cerevisiae* regulates its expression by binding to RPS14B pre-mRNA and to 18S rRNA. *Mol Cell Biol* **19**, 826-834
44. Warner, J. R., and McIntosh, K. B. (2009) How common are extraribosomal functions of ribosomal proteins? *Mol Cell* **34**, 3-11
45. Lindstrom, M. S. (2009) Emerging functions of ribosomal proteins in gene-specific transcription and translation. *Biochem Biophys Res Commun* **379**, 167-170
46. Kapasi, P., Chaudhuri, S., Vyas, K., Baus, D., Komar, A. A., Fox, P. L., Merrick, W. C., and Mazumder, B. (2007) L13a blocks 48S assembly: role of a general initiation factor in mRNA-specific translational control. *Mol Cell* **25**, 113-126
47. Pöll, G., Braun, T., Jakovljevic, J., Neueder, A., Jakob, S., Woolford, J. L., Jr., Tschochner, H., and Milkereit, P. (2009) rRNA maturation in yeast cells depleted of large ribosomal subunit proteins. *PLoS One* **4**, e8249
48. Ferreira-Cerca, S., Pöll, G., Gleizes, P. E., Tschochner, H., and Milkereit, P. (2005) Roles of eukaryotic ribosomal proteins in maturation and transport of pre-18S rRNA and ribosome function. *Mol Cell* **20**, 263-275
49. Kruiswijk, T., Planta, R. J., and Krop, J. M. (1978) The course of the assembly of ribosomal subunits in yeast. *Biochim Biophys Acta* **517**, 378-389
50. Lastick, S. M. (1980) The assembly of ribosomes in HeLa cell nucleoli. *Eur J Biochem* **113**, 175-182
51. Schäfer, T., Strauss, D., Petfalski, E., Tollervey, D., and Hurt, E. (2003) The path from nucleolar 90S to cytoplasmic 40S pre-ribosomes. *EMBO J* **22**, 1370-1380
52. Nissan, T. A., Bassler, J., Petfalski, E., Tollervey, D., and Hurt, E. (2002) 60S pre-ribosome formation viewed from assembly in the nucleolus until export to the cytoplasm. *EMBO J* **21**, 5539-5547
53. Grandi, P., Rybin, V., Bassler, J., Petfalski, E., Strauss, D., Marzioch, M., Schäfer, T., Kuster, B., Tschochner, H., Tollervey, D., Gavin, A. C., and Hurt, E. (2002) 90S pre-ribosomes

include the 35S pre-rRNA, the U3 snoRNP, and 40S subunit processing factors but predominantly lack 60S synthesis factors. *Mol Cell* **10**, 105-115
54. Ferreira-Cerca, S., Pöll, G., Kuhn, H., Neueder, A., Jakob, S., Tschochner, H., and Milkereit, P. (2007) Analysis of the *in vivo* assembly pathway of eukaryotic 40S ribosomal proteins. *Mol Cell* **28**, 446-457
55. Zhang, J., Harnpicharnchai, P., Jakovljevic, J., Tang, L., Guo, Y., Oeffinger, M., Rout, M. P., Hiley, S. L., Hughes, T., and Woolford, J. L., Jr. (2007) Assembly factors Rpf2 and Rrs1 recruit 5S rRNA and ribosomal proteins rpL5 and rpL11 into nascent ribosomes. *Genes Dev* **21**, 2580-2592
56. West, M., Hedges, J. B., Chen, A., and Johnson, A. W. (2005) Defining the order in which Nmd3p and Rpl10p load onto nascent 60S ribosomal subunits. *Mol Cell Biol* **25**, 3802-3813
57. Sahasranaman, A., Dembowski, J., Strahler, J., Andrews, P., Maddock, J., and Woolford, J. L., Jr. (2011) Assembly of *Saccharomyces cerevisiae* 60S ribosomal subunits: role of factors required for 27S pre-rRNA processing. *EMBO J* **30**, 4020-4032
58. Saveanu, C., Namane, A., Gleizes, P. E., Lebreton, A., Rousselle, J. C., Noaillac-Depeyre, J., Gas, N., Jacquier, A., and Fromont-Racine, M. (2003) Sequential protein association with nascent 60S ribosomal particles. *Mol Cell Biol* **23**, 4449-4460
59. Babiano, R., Gamalinda, M., Woolford, J. L., Jr., and de la Cruz, J. (2012) *Saccharomyces cerevisiae* ribosomal protein L26 is not essential for ribosome assembly and function. *Mol Cell Biol*
60. Babiano, R., and de la Cruz, J. (2010) Ribosomal protein L35 is required for 27SB pre-rRNA processing in *Saccharomyces cerevisiae Nucleic Acids Res* **38**, 5177-5192
61. Rodríguez-Mateos, M., García-Gómez, J. J., Francisco-Velilla, R., Remacha, M., de la Cruz, J., and Ballesta, J. P. G. (2009) Role and dynamics of the ribosomal protein P0 and its related *trans*-acting factor Mrt4 during ribosome assembly in *Saccharomyces cerevisiae*. *Nucleic Acids Res* **37**, 7519-7532
62. Rosado, I. V., Kressler, D., and de la Cruz, J. (2007) Functional analysis of *Saccharomyces cerevisiae* ribosomal protein Rpl3p in ribosome synthesis. *Nucleic Acids Res* **35**, 4203-4213
63. Wu, B., Lukin, J., Yee, A., Lemak, A., Semesi, A., Ramelot, T. A., Kennedy, M. A., and Arrowsmith, C. H. (2008) Solution structure of ribosomal protein L40E, a unique C4 zinc finger protein encoded by archaeon *Sulfolobus solfataricus*. *Protein Sci* **17**, 589-596
64. Nakao, A., Yoshihama, M., and Kenmochi, N. (2004) RPG: the Ribosomal Protein Gene database. *Nucleic Acids Res* **32**, D168-170
65. Chan, Y. L., Suzuki, K., and Wool, I. G. (1995) The carboxyl extensions of two rat ubiquitin fusion proteins are ribosomal proteins S27a and L40. *Biochem Biophys Res Commun* **215**, 682-690
66. Finley, D., Bartel, B., and Varshavsky, A. (1989) The tails of ubiquitin precursors are ribosomal proteins whose fusion to ubiquitin facilitates ribosome biogenesis. *Nature* **338**, 394-401
67. Lacombe, T., García-Gómez, J. J., de la Cruz, J., Roser, D., Hurt, E., Linder, P., and Kressler, D. (2009) Linear ubiquitin fusion to Rps31 and its subsequent cleavage are required for the efficient production and functional integrity of 40S ribosomal subunits. *Mol Microbiol* **72**, 69-84
68. Gómez-Lorenzo, M. G., and García-Bustos, J. F. (1998) Ribosomal P-protein stalk function is targeted by sordarin antifungals. *J Biol Chem* **273**, 25041-25044
69. Justice, M. C., Hsu, M. J., Tse, B., Ku, T., Balkovec, J., Schmatz, D., and Nielsen, J. (1998) Elongation factor 2 as a novel target for selective inhibition of fungal protein synthesis. *J Biol Chem* **273**, 3148-3151
70. Capa, L., Mendoza, A., Lavandera, J. L., Gomez de las Heras, F., and Garcia-Bustos, J. F. (1998) Translation elongation factor 2 is part of the target for a new family of antifungals. *Antimicrob Agents Chemother* **42**, 2694-2699
71. Wach, A., Brachat, A., Pöhlmann, R., and Philippsen, P. (1994) New heterologous modules for classical or PCR-based gene disruptions in *Saccharomyces cerevisiae*. *Yeast* **10**, 1793-1808
72. Kaiser, C., Michaelis, S., and Mitchell, A. (1994) *Methods in yeast genetics: a Cold Spring Harbor Laboratory course manual*, Cold Spring Harbor Laboratory Press, Cold Spring Harbor, N. Y.

73. Sambrook, J., Fritsch, E. F., and Maniatis, T. (1989) *Molecular cloning: a laboratory manual*, 2nd ed., Cold Spring Harbor Laboratory Press, Cold Spring Harbor, N. Y.
74. Gietz, R. D., and Sugino, A. (1988) New yeast-*Escherichia coli* shuttle vectors constructed with in vitro mutagenized yeast genes lacking six-base pair restriction sites. *Gene* **74**, 527-534
75. Schmidt, A., Bickle, M., Beck, T., and Hall, M. N. (1997) The yeast phosphatidylinositol kinase homolog TOR2 activates RHO1 and RHO2 via the exchange factor ROM2. *Cell* **88**, 531-542
76. Rosado, I. V., and de la Cruz, J. (2004) Npa1p is an essential trans-acting factor required for an early step in the assembly of 60S ribosomal subunits in *Saccharomyces cerevisiae*. *RNA* **10**, 1073-1083
77. Kressler, D., de la Cruz, J., Rojo, M., and Linder, P. (1997) Fal1p is an essential DEAD-box protein involved in 40S-ribosomal-subunit biogenesis in *Saccharomyces cerevisiae*. *Mol Cell Biol* **17**, 7283-7294
78. Vilella, M. D., Remacha, M., Ortiz, B. L., Mendez, E., and Ballesta, J. P. (1991) Characterization of the yeast acidic ribosomal phosphoproteins using monoclonal antibodies. Proteins L44/L45 and L44' have different functional roles. *Eur J Biochem* **196**, 407-414
79. Rodríguez-Mateos, M., Abia, D., García-Gómez, J. J., Morreale, A., de la Cruz, J., Santos, C., Remacha, M., and Ballesta, J. P. G. (2009) The amino terminal domain from Mrt4 protein can functionally replace the RNA binding domain of the ribosomal P0 protein. *Nucleic Acids Res* **37**, 3514-3521
80. Petitjean, A., Bonneaud, N., and Lacroute, F. (1995) The duplicated *Saccharomyces cerevisiae* gene *SSM1* encodes a eucaryotic homolog of the eubacterial and archeabacterial L1 ribsomal protein. *Mol Cell Biol* **15**, 5071-5081
81. Zanelli, C. F., Maragno, A. L., Gregio, A. P., Komili, S., Pandolfi, J. R., Mestriner, C. A., Lustri, W. R., and Valentini, S. R. (2006) eIF5A binds to translational machinery components and affects translation in yeast. *Biochem Biophys Res Commun* **348**, 1358-1366
82. Eisinger, D. P., Dick, F. A., and Trumpower, B. L. (1997) Qsr1p, a 60S ribosomal subunit protein, is required for joining of 40S and 60S subunits. *Mol Cell Biol* **17**, 5136-5145
83. Frey, S., Pool, M., and Seedorf, M. (2001) Scp160p, an RNA-binding, polysome-associated protein, localizes to the endoplasmic reticulum of *Saccharomyces cerevisiae* in a microtubule-dependent manner. *J Biol Chem* **276**, 15905-15912
84. Emery, B., de la Cruz, J., Rocak, S., Deloche, O., and Linder, P. (2004) Has1p, a member of the DEAD-box family, is required for 40S ribosomal subunit biogenesis in *Saccharomyces cerevisiae*. *Mol Microbiol* **52**, 141-158
85. Ausubel, F. M., Brent, R., Kingston, R. E., Moore, D. D., Seidman, J. G., Smith, J. A., and Struhl, K. (1994) *Saccharomyces cerevisiae*. in *Current Protocols in Molecular Biology*, John Wiley & Sons, Inc., New York, N. Y. pp 13.10.11-13.14.17
86. Venema, J., Planta, R. J., and Raué, H. A. (1998) *In vivo* mutational analysis of ribosomal RNA in *Saccharomyces cerevisiae*. in *Protein synthesis: Methods and protocols* (Martin, R. ed.), Humana Press, Totowa, N. J. pp 257-270
87. Rosado, I. V., Dez, C., Lebaron, S., Caizergues-Ferrer, M., Henry, Y., and de la Cruz, J. (2007) Characterization of *Saccharomyces cerevisiae* Npa2p (Urb2p) reveals a low-molecular-mass complex containing Dbp6p, Npa1p (Urb1p), Nop8p, and Rsa3p involved in early steps of 60S ribosomal subunit biogenesis. *Mol Cell Biol* **27**, 1207-1221
88. Kressler, D., de la Cruz, J., Rojo, M., and Linder, P. (1998) Dbp6p is an essential putative ATP-dependent RNA helicase required for 60S-ribosomal-subunit assembly in *Saccharomyces cerevisiae*. *Mol Cell Biol* **18**, 1855-1865
89. Dez, C., Froment, C., Noaillac-Depeyre, J., Monsarrat, B., Caizergues-Ferrer, M., and Henry, Y. (2004) Npa1p, a component of very early pre-60S ribosomal particles, associates with a subset of small nucleolar RNPs required for peptidyl transferase center modification. *Mol Cell Biol* **24**, 6324-6337
90. García-Gómez, J. J., Lebaron, S., Froment, C., Monsarrat, B., Henry, Y., and de la Cruz, J. (2011) Dynamics of the putative RNA helicase Spb4 during ribosome assembly in Saccharomyces cerevisiae. *Mol Cell Biol* **31**, 4156-4164
91. Ulbrich, C., Diepholz, M., Bassler, J., Kressler, D., Pertschy, B., Galani, K., Bottcher, B., and Hurt, E. (2009) Mechanochemical removal of ribosome biogenesis factors from nascent 60S ribosomal subunits. *Cell* **138**, 911-922

92. Belk, J. P., He, F., and Jacobson, A. (1999) Overexpression of truncated Nmd3p inhibits protein synthesis in yeast. *RNA* **5**, 1055-1070
93. Valerio-Santiago, M., and Monje-Casas, F. (2011) Tem1 localization to the spindle pole bodies is essential for mitotic exit and impairs spindle checkpoint function. *J Cell Biol* **192**, 599-614
94. Segref, A., Sharma, K., Doye, V., Hellwig, A., Huber, J., Luhrmann, R., and Hurt, E. (1997) Mex67p, a novel factor for nuclear mRNA export, binds to both poly(A)+ RNA and nuclear pores. *EMBO J* **16**, 3256-3271
95. Hedges, J., West, M., and Johnson, A. W. (2005) Release of the export adapter, Nmd3p, from the 60S ribosomal subunit requires Rpl10p and the cytoplasmic GTPase Lsg1p. *EMBO J* **24**, 567-579
96. Menne, T. F., Goyenechea, B., Sanchez-Puig, N., Wong, C. C., Tonkin, L. M., Ancliff, P. J., Brost, R. L., Costanzo, M., Boone, C., and Warren, A. J. (2007) The Shwachman-Bodian-Diamond syndrome protein mediates translational activation of ribosomes in yeast. *Nature Genet* **39**, 486-495
97. Mager, W. H., Planta, R. J., Ballesta, J.-P. G., Lee, J. C., Mizuta, K., Suzuki, K., Warner, J. R., and Woolford, J. (1997) A new nomenclature for the cytoplasmic ribosomal proteins of *Saccharomyces cerevisiae*. *Nucleic Acids Res* **25**, 4872-4875
98. Ozkaynak, E., Finley, D., Solomon, M. J., and Varshavsky, A. (1987) The yeast ubiquitin genes: a family of natural gene fusions. *EMBO J* **6**, 1429-1439
99. Steffen, K. K., McCormick, M. A., Pham, K. M., Mackay, V. L., Delaney, J. R., Murakami, C. J., Kaeberlein, M., and Kennedy, B. K. (2012) Ribosome deficiency protects against ER stress in *Saccharomyces cerevisiae*. *Genetics* **191**, 107-118
100. Holstege, F. C., Jennings, E. G., Wyrick, J. J., Lee, T. I., Hengartner, C. J., Green, M. R., Golub, T. R., Lander, E. S., and Young, R. A. (1998) Dissecting the regulatory circuitry of a eukaryotic genome. *Cell* **95**, 717-728
101. Komili, S., Farny, N. G., Roth, F. P., and Silver, P. A. (2007) Functional specificity among ribosomal proteins regulates gene expression. *Cell* **131**, 557-571
102. Stage-Zimmermann, T., Schmidt, U., and Silver, P. A. (2000) Factors affecting nuclear export of the 60S ribosomal subunit *in vivo*. *Mol Biol Cell* **11**, 3777-3789
103. Lo, K. Y., Li, Z., Bussiere, C., Bresson, S., Marcotte, E. M., and Johnson, A. W. (2010) Defining the pathway of cytoplasmic maturation of the 60S ribosomal subunit. *Mol Cell* **39**, 196-208
104. Kemmler, S., Occhipinti, L., Veisu, M., and Panse, V. G. (2009) Yvh1 is required for a late maturation step in the 60S biogenesis pathway. *J Cell Biol* **186**, 863-880
105. Kosugi, S., Hasebe, M., Tomita, M., and Yanagawa, H. (2009) Systematic identification of cell cycle-dependent yeast nucleocytoplasmic shuttling proteins by prediction of composite motifs. *Proc Natl Acad Sci USA* **106**, 10171-10176
106. Ho, J. H.-N., Kallstrom, G., and Johnson, A. W. (2000) Nmd3p is a Crm1p-dependent adapter protein for nuclear export of the large ribosomal subunit. *J Cell Biol* **151**, 1057-1066
107. Hackmann, A., Gross, T., Baierlein, C., and Krebber, H. (2011) The mRNA export factor Npl3 mediates the nuclear export of large ribosomal subunits. *EMBO Rep* **12**, 1024-1031
108. Yao, Y., Demoinet, E., Saveanu, C., Lenormand, P., Jacquier, A., and Fromont-Racine, M. (2010) Ecm1 is a new pre-ribosomal factor involved in pre-60S particle export. *RNA* **16**, 1007-1017
109. Yao, W., Roser, D., Kohler, A., Bradatsch, B., Bassler, J., and Hurt, E. (2007) Nuclear export of ribosomal 60S subunits by the general mRNA export receptor Mex67-Mtr2. *Mol Cell* **26**, 51-62
110. Bradatsch, B., Katahira, J., Kowalinski, E., Bange, G., Yao, W., Sekimoto, T., Baumgartel, V., Boese, G., Bassler, J., Wild, K., Peters, R., Yoneda, Y., Sinning, I., and Hurt, E. (2007) Arx1 functions as an unorthodox nuclear export receptor for the 60S preribosomal subunit. *Mol Cell* **27**, 767-779
111. Hung, N. J., Lo, K. Y., Patel, S. S., Helmke, K., and Johnson, A. W. (2008) Arx1 is a nuclear export receptor for the 60S ribosomal subunit in yeast. *Mol Biol Cell* **19**, 735-744
112. Gadal, O., Strauss, D., Kessl, J., Trumpower, B., Tollervey, D., and Hurt, E. (2001) Nuclear export of 60S ribosomal subunit depends on Xpo1p and requires a nuclear export sequence-

containing factor, Nmd3p, that associates with the large subunit protein Rpl10p. *Mol Cell Biol* **21**, 3405-3415
113. Hurt, E., Hannus, S., Schmelzl, B., Lau, D., Tollervey, D., and Simos, G. (1999) A novel *in vivo* assay reveals inhibition of ribosomal nuclear export in Ran-cycle and nucleoporin mutants. *J Cell Biol* **144**, 389-401
114. Dragon, F., Gallagher, J. E., Compagnone-Post, P. A., Mitchell, B. M., Porwancher, K. A., Wehner, K. A., Wormsley, S., Settlage, R. E., Shabanowitz, J., Osheim, Y., Beyer, A. L., Hunt, D. F., and Baserga, S. J. (2002) A large nucleolar U3 ribonucleoprotein required for 18S ribosomal RNA biogenesis. *Nature* **417**, 967-970
115. Kallstrom, G., Hedges, J., and Johnson, A. (2003) The putative GTPases Nog1p and Lsg1p are required for 60S ribosomal subunit biogenesis and are localized to the nucleus and cytoplasm, respectively. *Mol Cell Biol* **23**, 4344-4355
116. Kressler, D., Roser, D., Pertschy, B., and Hurt, E. (2008) The AAA ATPase Rix7 powers progression of ribosome biogenesis by stripping Nsa1 from pre-60S particles. *J Cell Biol* **181**, 935-944
117. Harnpicharnchai, P., Jakovljevic, J., Horsey, E., Miles, T., Roman, J., Rout, M., Meagher, D., Imai, B., Guo, Y., Brame, C. J., Shabanowitz, J., Hunt, D. F., and Woolford, J. L., Jr. (2001) Composition and functional characterization of yeast 66S ribosome assembly intermediates. *Mol Cell* **8**, 505-515
118. Wehner, K. A., and Baserga, S. J. (2002) The sigma(70)-like motif: a eukaryotic RNA binding domain unique to a superfamily of proteins required for ribosome biogenesis. *Mol Cell* **9**, 329-339
119. Fatica, A., Cronshaw, A. D., Dlakic, M., and Tollervey, D. (2002) Ssf1p prevents premature processing of an early pre-60S ribosomal particle. *Mol Cell* **9**, 341-351
120. Santos, C., and Ballesta, J. P. G. (1994) Ribosomal protein P0, contrary to phosphoproteins P1 and P2, is required for ribosome activity and *Saccharomyces cerevisiae* viability. *J Biol Chem* **269**, 15689-15696
121. Oeffinger, M. (2010) Joining the interface: a site for Nmd3 association on 60S ribosome subunits. *J Cell Biol* **189**, 1071-1073
122. Sengupta, J., Bussiere, C., Pallesen, J., West, M., Johnson, A. W., and Frank, J. (2010) Characterization of the nuclear export adaptor protein Nmd3 in association with the 60S ribosomal subunit. *J Cell Biol* **189**, 1079-1086
123. Gartmann, M., Blau, M., Armache, J. P., Mielke, T., Topf, M., and Beckmann, R. (2010) Mechanism of eIF6-mediated inhibition of ribosomal subunit joining. *J Biol Chem* **285**, 14848-14851
124. Senger, B., Lafontaine, D. L., Graindorge, J. S., Gadal, O., Camasses, A., Sanni, A., Garnier, J. M., Breitenbach, M., Hurt, E., and Fasiolo, F. (2001) The nucle(ol)ar Tif6p and Efl1p are required for a late cytoplasmic step of ribosome synthesis. *Mol Cell* **8**, 1363-1373
125. Hedges, J., Chen, Y. I., West, M., Bussiere, C., and Johnson, A. W. (2006) Mapping the functional domains of yeast NMD3, the nuclear export adapter for the 60 S ribosomal subunit. *J Biol Chem* **281**, 36579-36587
126. Bussiere, C., Hashem, Y., Arora, S., Frank, J., and Johnson, A. W. (2012) Integrity of the P-site is probed during maturation of the 60S ribosomal subunit. *J Cell Biol* **197**, 747-759
127. Spahn, C. M., Gomez-Lorenzo, M. G., Grassucci, R. A., Jorgensen, R., Andersen, G. R., Beckmann, R., Penczek, P. A., Ballesta, J. P., and Frank, J. (2004) Domain movements of elongation factor eEF2 and the eukaryotic 80S ribosome facilitate tRNA translocation. *EMBO J* **23**, 1008-1119
128. Botet, J., Rodriguez-Mateos, M., Ballesta, J. P., Revuelta, J. L., and Remacha, M. (2008) A chemical genomic screen in *Saccharomyces cerevisiae* reveals a role for diphthamidation of translation elongation factor 2 in inhibition of protein synthesis by sordarin. *Antimicrob Agents Chemother* **52**, 1623-1629
129. Justice, M. C., Ku, T., Hsu, M. J., Carniol, K., Schmatz, D., and Nielsen, J. (1999) Mutations in ribosomal protein L10e confer resistance to the fungal-specific eukaryotic elongation factor 2 inhibitor sordarin. *J Biol Chem* **274**, 4869-4875
130. Horiguchi, G., Molla-Morales, A., Perez-Perez, J. M., Kojima, K., Robles, P., Ponce, M. R., Micol, J. L., and Tsukaya, H. (2011) Differential contributions of ribosomal protein genes to *Arabidopsis thaliana* leaf development. *Plant J* **65**, 724-736

131. Xue, S., and Barna, M. (2012) Specialized ribosomes: a new frontier in gene regulation and organismal biology. *Nat Rev Mol Cell Biol* **13**, 355-369
132. Baronas-Lowell, D. M., and Warner, J. R. (1990) Ribosomal protein L30 is dispensable in the yeast *Saccharomyces cerevisiae*. *Mol Cell Biol* **10**, 5235-5243
133. McIntosh, K. B., Bhattacharya, A., Willis, I. M., and Warner, J. R. (2011) Eukaryotic cells producing ribosomes deficient in Rpl1 are hypersensitive to defects in the ubiquitin-proteasome system. *PLoS One* **6**, e23579
134. Gadal, O., Strauss, D., Braspenning, J., Hoepfner, D., Petfalski, E., Philippsen, P., Tollervey, D., and Hurt, E. (2001) A nuclear AAA-type ATPase (Rix7p) is required for biogenesis and nuclear export of 60S ribosomal subunits. *EMBO J* **20**, 3695-3704
135. Lo, K. Y., Li, Z., Wang, F., Marcotte, E. M., and Johnson, A. W. (2009) Ribosome stalk assembly requires the dual-specificity phosphatase Yvh1 for the exchange of Mrt4 with P0. *J Cell Biol* **186**, 849-862
136. Lebreton, A., Saveanu, C., Decourty, L., Rain, J. C., Jacquier, A., and Fromont-Racine, M. (2006) A functional network involved in the recycling of nucleocytoplasmic pre-60S factors. *J Cell Biol* **173**, 349-360
137. Pertschy, B., Saveanu, C., Zisser, G., Lebreton, A., Tengg, M., Jacquier, A., Liebminger, E., Nobis, B., Kappel, L., van der Klei, I., Hogenauer, G., Fromont-Racine, M., and Bergler, H. (2007) Cytoplasmic recycling of 60S preribosomal factors depends on the AAA protein Drg1. *Mol Cell Biol* **27**, 6581-6592
138. Wilson, D. N., and Nierhaus, K. H. (2005) Ribosomal proteins in the spotlight. *Crit Rev Biochem Mol Biol* **40**, 243-267
139. Petrov, A. N., Meskauskas, A., Roshwalb, S. C., and Dinman, J. D. (2008) Yeast ribosomal protein L10 helps coordinate tRNA movement through the large subunit. *Nucleic Acids Res* **36**, 6187-6198
140. Briones, C., and Ballesta, J. P. G. (2000) Conformational changes induced in the *Saccharomyces cerevisiae* GTPase-associated rRNA by ribosomal stalk components and a translocator inhibitor. *Nucleic Acids Res* **28**, 4497-4505
141. Meskauskas, A., Russ, J. R., and Dinman, J. D. (2008) Structure/function analysis of yeast ribosomal protein L2. *Nucleic Acids Res* **36**, 1826-1835
142. Rhodin, M. H., Rakauskaite, R., and Dinman, J. D. (2011) The central core region of yeast ribosomal protein L11 is important for subunit joining and translational fidelity. *Mol Genet Genomics* **285**, 505-516
143. Martín-Marcos, P., Hinnebusch, A. G., and Tamame, M. (2007) Ribosomal protein L33 is required for ribosome biogenesis, subunit joining, and repression of *GCN4* translation. *Mol Cell Biol* **27**, 5968-5985
144. Ho, J. H.-N., Kallstrom, G., and Johnson, A. W. (2000) Nascent 60S ribosomal subunits enter the free pool bound by Nmd3p. *RNA* **6**, 1625-1634
145. Santos, C., Rodriguez-Gabriel, M. A., Remacha, M., and Ballesta, J. P. (2004) Ribosomal P0 protein domain involved in selectivity of antifungal sordarin derivatives. *Antimicrob Agents Chemother* **48**, 2930-2936
146. Bécam, A. M., Nasr, F., Racki, W. J., Zagulski, M., and Herbert, C. J. (2001) Ria1p (Ynl163c), a protein similar to elongation factors 2, is involved in the biogenesis of the 60S subunit of the ribosome in *Saccharomyces cerevisiae*. *Mol Genet Genomics* **266**, 454-462
147. Pettersen, E. F., Goddard, T. D., Huang, C. C., Couch, G. S., Greenblatt, D. M., Meng, E. C., and Ferrin, T. E. (2004) UCSF Chimera-a visualization system for exploratory research and analysis. *J Comput Chem* **25**, 1605-1612
148. Cannone, J. J., Subramanian, S., Schnare, M. N., Collett, J. R., D'Souza, L. M., Du, Y., Feng, B., Lin, N., Madabusi, L. V., Muller, K. M., Pande, N., Shang, Z., Yu, N., and Gutell, R. R. (2002) The comparative RNA web (CRW) site: an online database of comparative sequence and structure information for ribosomal, intron, and other RNAs. *BMC Bioinformatics* **3**, 2

ACKNOWLEDGMENTS

We are indebted to the colleagues mentioned in the text for their gift of material used in this study. We also thank M. Carballo, L. Navarro and C. Reyes of the Biology Service (CITIUS) from the University of Seville for help with the phosphorimager analysis and F. Monje-Casas for valuable advice on immunofluorescence experiments and J.P.G. Ballesta on sordarin assays. This work was

supported by grants from the Spanish Ministry of Science and Innovation (MICINN) and FEDER (BFU2010-15690) and the Andalusian Government (CVI-271, P08-CVI-03508) to J.d.l.C. and from the Swiss National Science Foundation (PP00P3_123341) to D.K. A.F.-P. is a recipient of a PIF fellowship from the University of Seville.

FOOTNOTES

The abbreviations used are: 50% inhibitory concentration, IC_{50}; eEF, eukaryotic elongation factor; GAC, GTPase-associated center; HA, hemaglutinin, NLS, nuclear localisation signal; ORF, open reading frame; pre-rRNA, precursor rRNA; PTC, peptidyl-transferase center; r-protein, ribosomal protein; rRNA, ribosomal RNA; SD, synthetic dextrose (minimal medium containing glucose); SRL, sarcin-ricin loop; YPD, yeast extract-peptone-dextrose (rich medium containing glucose).

FIGURE LEGENDS

FIGURE 1. Growth and polysome profile analysis of the *rpl40a* and *rpl40b* null mutants. (A) Growth phenotypes of *rpl40* mutants. Strains W303-1A (*Wild-type*), JDY920 (*rpl40a*Δ) and JDY922 (*rpl40b*Δ), which carry a YCplac111 plasmid, were grown in minimal SD-Leu medium and diluted to an OD_{600} of 0.05. Cells were spotted in 10-fold serial dilutions onto SD-Leu plates and incubated at 30 ºC for 3 days. The doubling times in liquid SD-Leu at 30 ºC are indicated in minutes. Values correspond to the mean and the standard deviation of five independent experiments. (B) Polysome profiles of the above strains. These strains were grown in YPD medium at 30 ºC to an OD_{600} of around 0.8. Whole cell extracts were prepared and 10 A_{260} of each extract were resolved in 7-50% sucrose gradients. The A_{254} was continuously measured. Sedimentation is from left to right. The peaks of free 40S and 60S r-subunits, 80S free couples/monosomes and polysomes are indicated. Half-mers are labelled by arrows.

FIGURE 2. Analysis of the *GAL::RPL40* strain upon depletion of L40. (A) Growth comparison of the strains W303-1A (*Wild-type*) and JDY925 [pAS24-RPL40A] (*GAL::RPL40*). The cells were streaked on YPGal (Galactose) and YPD (Glucose) plates and incubated at 30 ºC for 3 days. (B) Growth curves of the wild-type (open circles) and *GAL::RPL40* (closed circles) cells at 30 ºC after shifting exponential cultures from liquid YPGal to liquid YPD medium for up to 12 h. Data are represented as the doubling time at the different times in YPD. (C) Polysome profile analysis of *GAL::RPL40* cells grown in YPGal or shifted for 12 h or 24 h to YPD. For details, see legend to Fig. 1*B*. The peaks of free 40S and 60S r-subunits, 80S free couples/monosomes and polysomes are indicated. Half-mers are labelled by arrows.

FIGURE 3. Depletion of L40 slightly delays 27SB pre-rRNA processing. (A) Strains W303-1A (*Wild-type*) and JDY925 [pAS24-RPL40A] (*GAL::RPL40*) were transformed with YCplac33 and then grown at 30 ºC in SGal-Ura and shifted for 12 h to SD-Ura. Cells were pulse-labelled with [5,6-^{3}H]uracil for 2 min and then chased with an excess of unlabelled uracil for the times indicated. Total RNA was extracted and 20,000 c.p.m. were loaded and separated on (A) a 1.2% agarose-6% formaldehyde gel or (B) a 7% polyacrylamide-8M urea, transferred to nylon membranes and visualized by fluorography. The positions of the different pre-rRNAs and mature rRNA are indicated.

FIGURE 4. Depletion of L40 does not significantly impair pre-rRNA processing. Strains W303-1A (*Wild-type*) and JDY925 [pAS24-RPL40A] (*GAL::RPL40*) were grown in YPGal at 30 ºC, shifted to YPD and harvested at the indicated times. Total RNA was extracted of each sample. Equal amount of total RNA (5 μg) was subjected to northern blot or primer extension analysis. (A) Northern blot analysis of high-molecular-mass pre- and mature rRNAs separated on a 1.2% agarose- 6% formaldehide gel. (B) Northern blot analysis of low-molecular-mass pre- and mature rRNAs separated on a 7% polyacrylamide- 8M urea gel. (C) Primer extension analysis of 27S and 25.5S pre-rRNAs. Probes used are indicated on the left of each panel between parentheses and described in Fig. S1*A* and Table S2. Signal intensities were measured by phosphorimager scanning; values (indicated below each lane) were normalised to those obtained for the wild-type control grown in YPGal and arbitrarily set at 1.0.

FIGURE 5. Depletion of L40 leads to nuclear retention of the 60S r-subunit reporter L25-eGFP. *GAL::RPL40* cells co-expressing Nop1-mRFP and either L25-eGFP or S3-eGFP from their cognate promoters, were grown at 30 ºC in SGal-Trp or shifted to SD-Trp for up to 9 h. The subcellular localisation of the GFP-tagged ribosomal proteins and the Nop1-mRFP nucleolar marker were analysed by fluorescence microscopy. Arrows point to nucleolar fluorescence. Approximately 200 cells were examined for each reporter and practically all cells gave the results shown in the pictures.

FIGURE 6. HA-tagged L40A protein assembles in the cytoplasm. Localisation of L25-eGFP, Nop1-mRFP and HA-L40A upon induction of the dominant negative *NMD3Δ100* allele; *rpl40* null cells expressing L25-eGFP and Nop1-mRFP from plasmid pRS314-RFP-NOP1-RPL25-eGFP and HA-L40A from plasmid YCplac111-UB-HA-RPL40A were transformed with the pRS316-GAL-NMΔ3Δ100 plasmid. Transformants were grown in SD-Leu-Ura-Trp or shifted for 24 h to SGal-Leu-Ura-Trp to fully induce the Nmd3Δ100 protein. The GFP and RFP signals were simultaneously inspected by fluorescence microscopy. Cells from the same cultures were also inspected by indirect immunofluorescence. HA-L40A was detected with monoclonal mouse anti-HA antibodies, followed by decoration with goat anti-mouse Cy3-coupled antibody. Chromatin DNA was stained with DAPI. Arrows point to either nucleolus or the nucleoplasm depending if Nop1-mRFP or DAPI was used as a marker, respectively. Approximately 200 cells were examined for each reporter and practically all cells gave the results shown in the pictures.

FIGURE 7. HA-L40A associates with almost mature pre-60S ribosomal particles. HA-tagged L40A was affinity purified with anti-HA antibodies as outlined in "Experimental Procedures" from total cell extracts of *rpl40* null cells expressing HA-L40A (HA-L40). Wild-type cells (L40) were used as an untagged L40 control. (A) Proteins were extracted from the pellets obtained after immunoprecipitation (lanes IP) or from an amount of total extracts corresponding to 0.5% of that used for purification (lanes T) and subjected to SDS-PAGE and western blotting using specific antibodies against the HA-tag, L1 and L35 r-proteins. (B) RNA was also extracted from the above IP and T samples and subjected to northern analysis of 7S pre-rRNA and mature 5.8S and 5S rRNAs. Probes, between parentheses, are described in Fig. S1*A* and Table S2.

FIGURE 8. HA-L40A protein assembles onto late cytoplasmic pre-60S ribosomal particles. The indicated GFP-tagged bait proteins were affinity purified by using the GFP-Trap®_A procedure (see "Experimental Procedures") from cells expressing HA-L40A from its cognate promotor. Cells not expressing a GFP-tagged bait protein were used as a negative control (None). Equivalent amounts of the corresponding purified complexes were separated on 4-12% gradient SDS-polyacrylamide gels and subjected to silver staining or western blot analysis using specific antibodies against the HA-epitope, the Nop1, Has1 and Mrt4 ribosome biogenesis factors and the L1 and L3 ribosomal proteins. Dots indicate the positions of bait proteins.

FIGURE 9. Localisation of L40 in the three-dimensional structure of the yeast 60S ribosomal subunit. (A) The position of the ribosomal proteins L3, L5, L9, L10, L11, L12, L20, L24, L40, P0, P1α and P2β are highlighted. The remaining ribosomal proteins are coloured in black and the rRNA in pale grey. The representation was generated with the UCSF Chimera program (147), using the atomic model for the crystal structure of the yeast 80S ribosome described by Ben-Shem *et al.* (PDB files 3U5I and 3U5H; (10)). (B) Close-up view of the position of L40 in the context of its binding site in the 60S ribosomal subunit. Only rRNA residues situated at or closer than 12 Å are shown (bases and phosphate backbone). Base numbering follows the 25S rRNA sequence deposited for the yeast 60S r-subunit (PDB file 3U5D; (10)), respectively. Selected residues are labelled in black. The N- and C-terminal ends of the L40 protein (I77 and K128, respectively) are also indicated. (C) Secondary structure of the GTPase-associated center (GAC), the peptidyltransferase center (PTC) and the sarcin-ricin loop region (SRL) from *S. cerevisiae* 25S rRNA domain II, V and VI, respectively. The structures, residue and helix (*H*) numbers were taken from The Comparative RNA Web Site (http: www.rrna.ccbb.utexas.edu) (148). Red circles indicate rRNA residues situated in close proximity of L40 (closer than 5 Å).

FIGURE 10. Nmd3 and Rlp24 are not properly recycled back to the nucleus upon depletion of L40. The *GAL::RPL40* strain, JDY925 [pAS24-RPL40A], was transformed with *CEN URA3* plasmids that

allow expression of GFP-tagged versions of either Arx1, Mex67, Mrt4, Nmd3, Rlp24 or Tif6. Cells were grown at 30 ºC in SGal-Leu-Ura (Gal) and shifted for 18 h to SD-Leu-Ura (18 h Glc). Then, the subcellular localization of these GFP-tagged proteins was examined by fluorescence microscopy. Arrows point to the nucle(ol)us. Approximately 200 cells were examined for each reporter. About 85% cells expressing GFP-tagged Nmd3 or Rlp24 showed full cytoplasmic fluorescence upon L40 depletion. Practically all cells gave the results shown in the pictures for remaining reporters.

FIGURE 11. Cells expressing the HA-tagged L40A are resistant to sordarin. Growth inhibition assays were performed in liquid YPD medium with or without different amounts of the sordarin derivative GM193663 in a microtiter format. The relative growth after incubation for 18 h at 30 ºC in the presence *versus* the absence of the antibiotic is the mean of four independent experiments. The strains evaluated were: W303-1A (*Wild-type*; open circles), JDY925 [YCplac33-UB-HA-RPL40A] (*HA-RPL40A*; closed circles), JDY919 (*rpl40aΔ*; open square), JDY922 (*rpl40bΔ*, open triangle), JDY711 (*rpl35bΔ*; open rhombus).

Figure 1- 1.5 columns

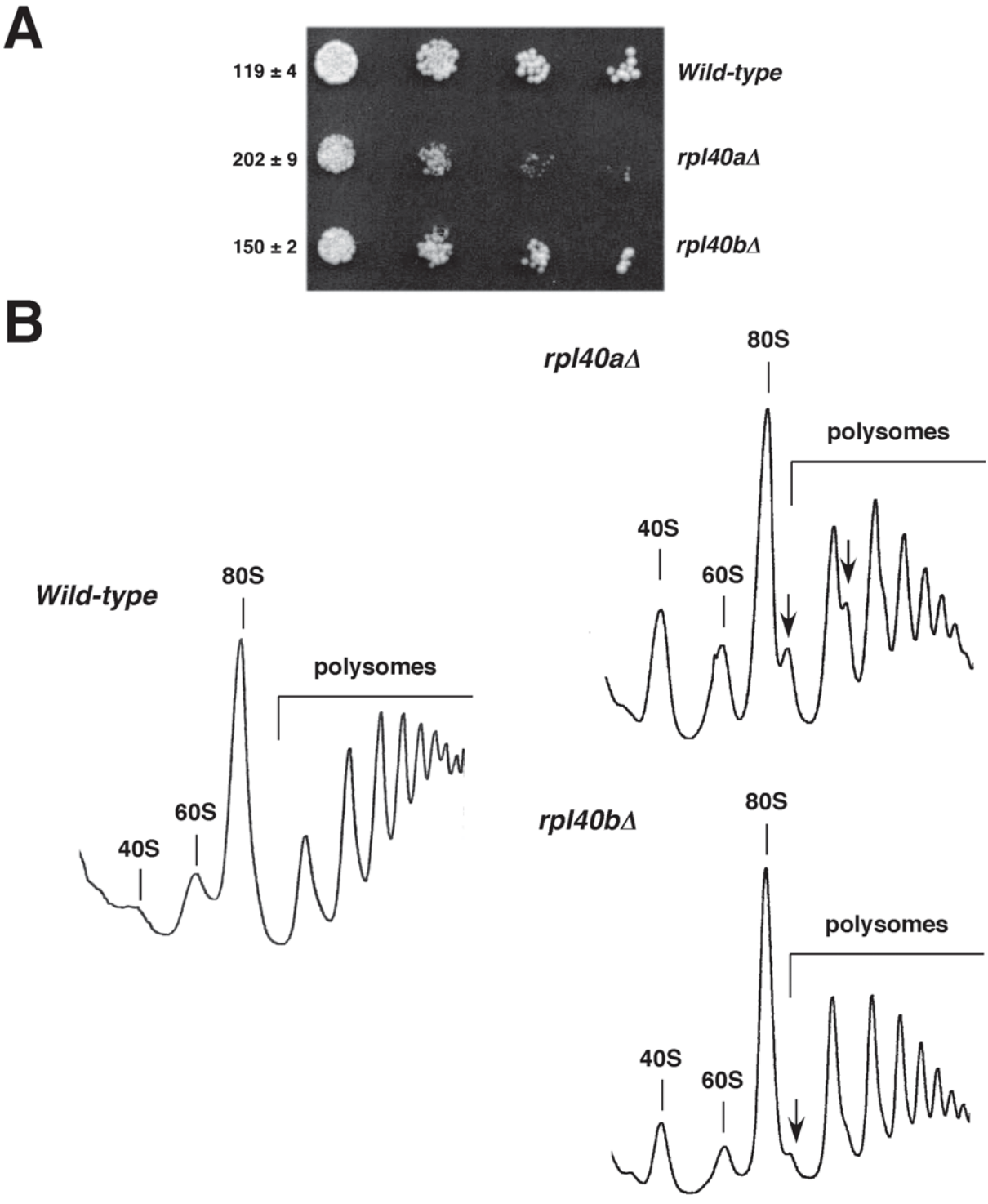

Figure 2- 2 columns

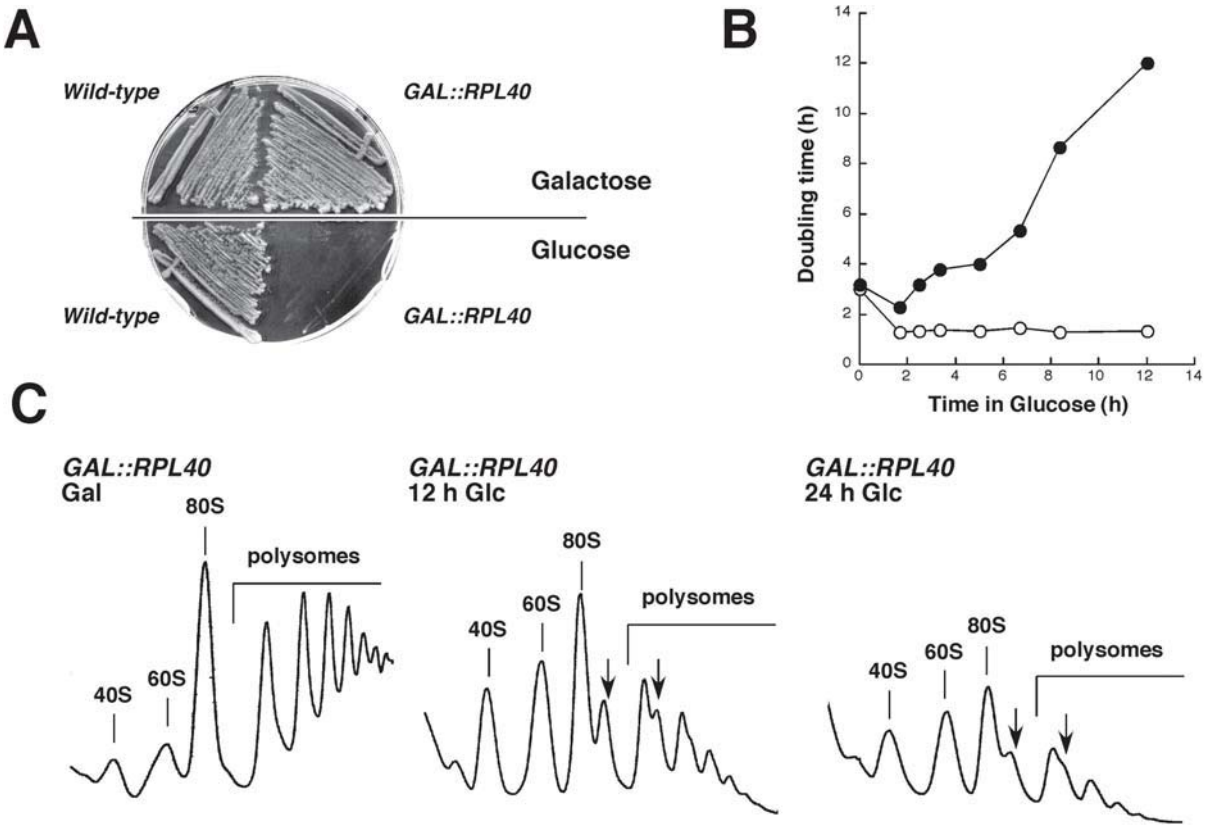

Figure 3- 1.5 columns

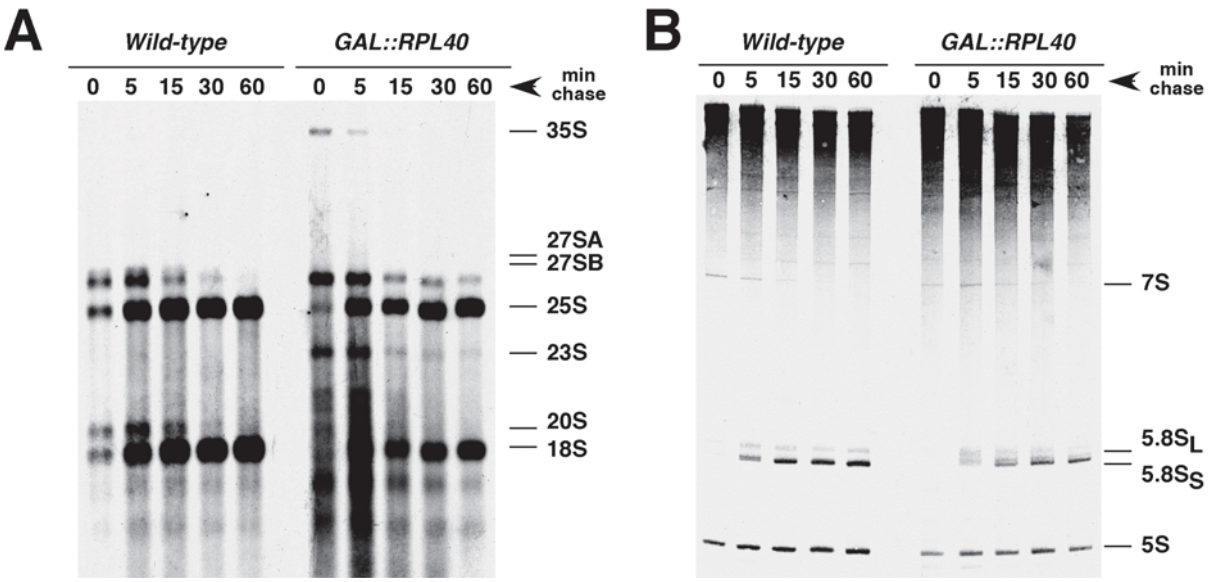

Figure 4- 1.5 columns

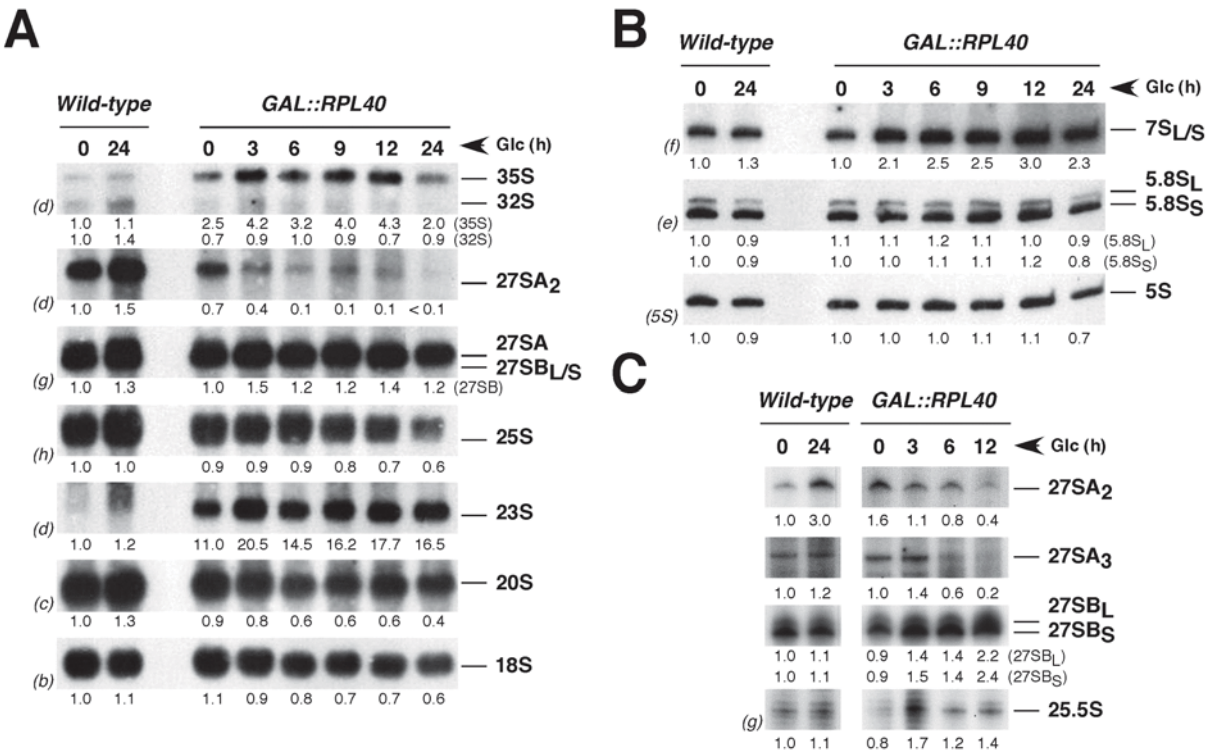

Figure 5- 1.5 columns

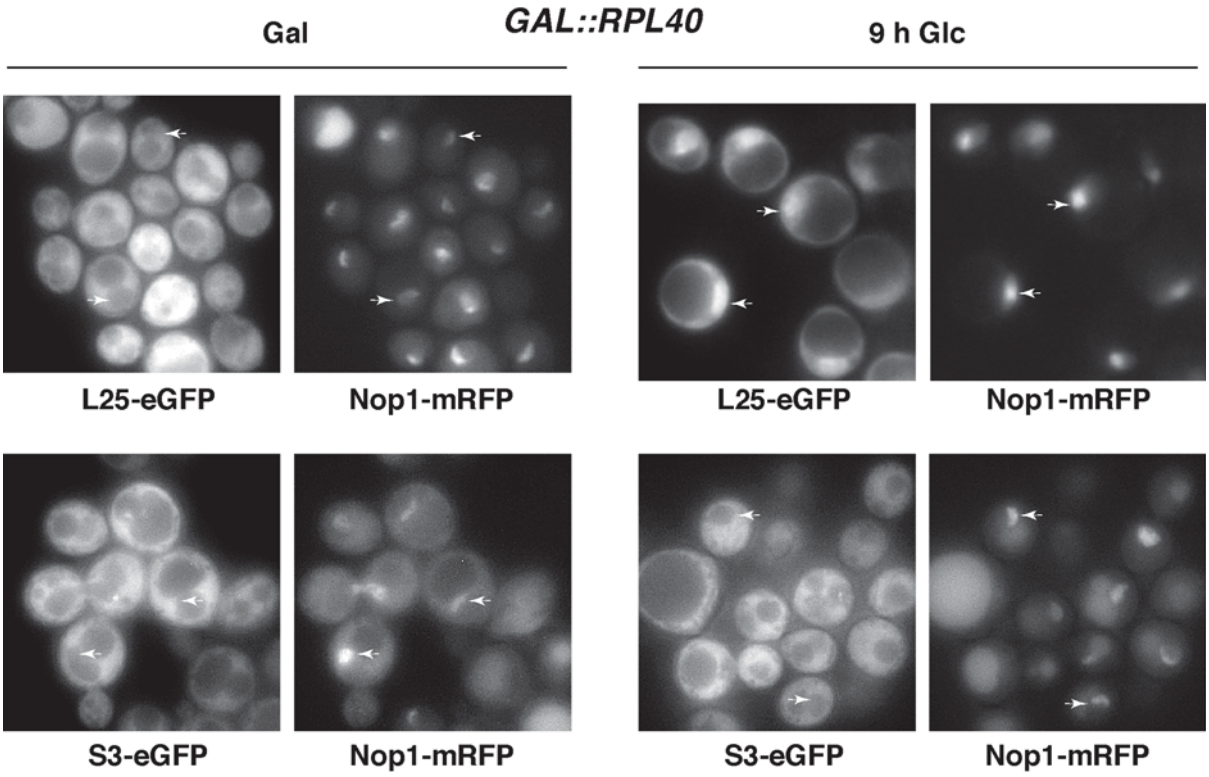

Figure 6- 1.5 columns

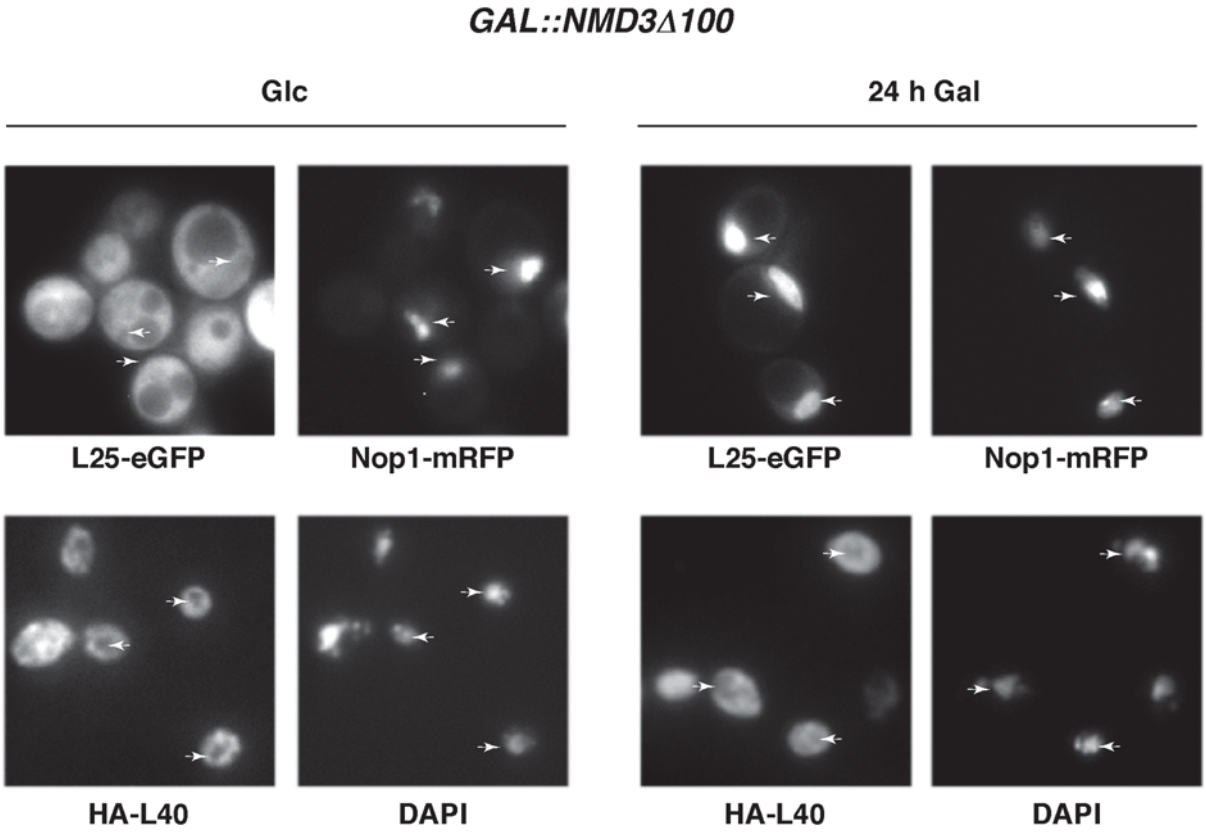

Figure 7- 1 column

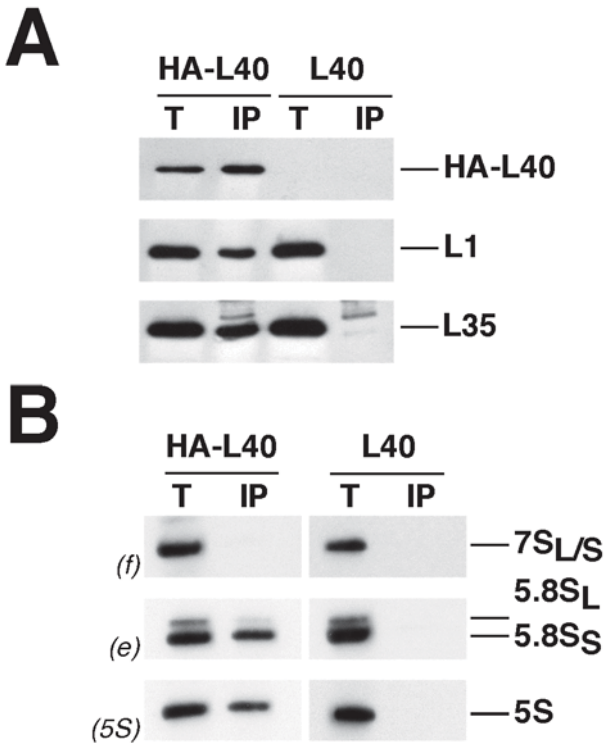

Figure 8- 1 column

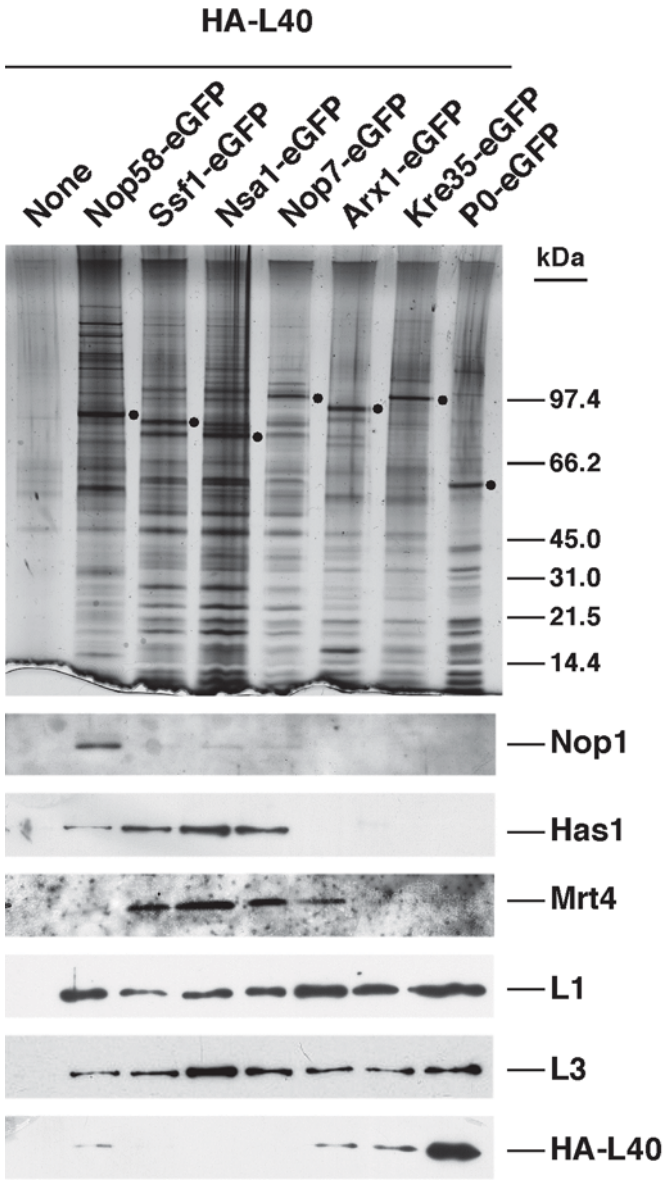

Figure 9- 2 columns

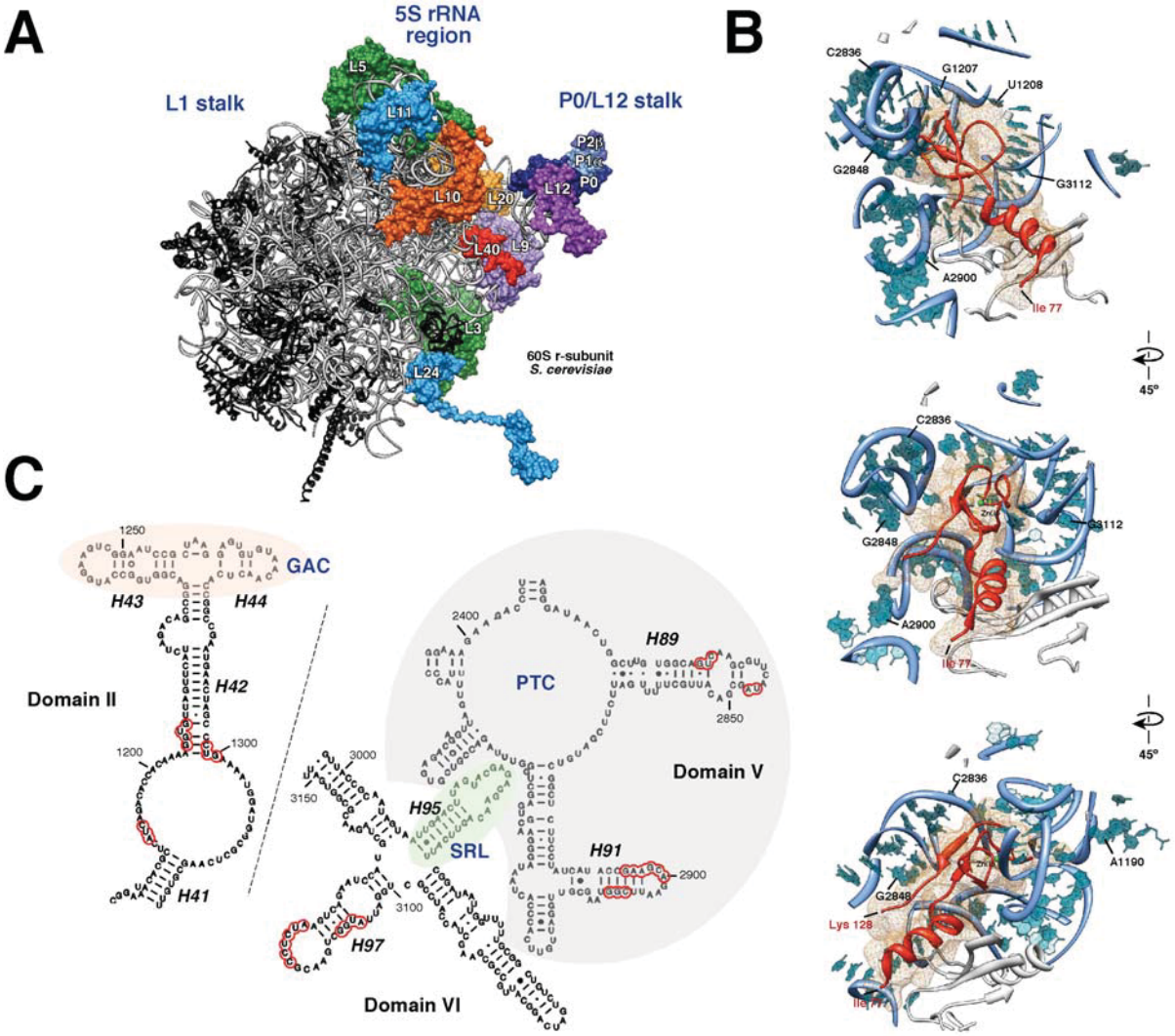

Figure 10- 1.5 columns

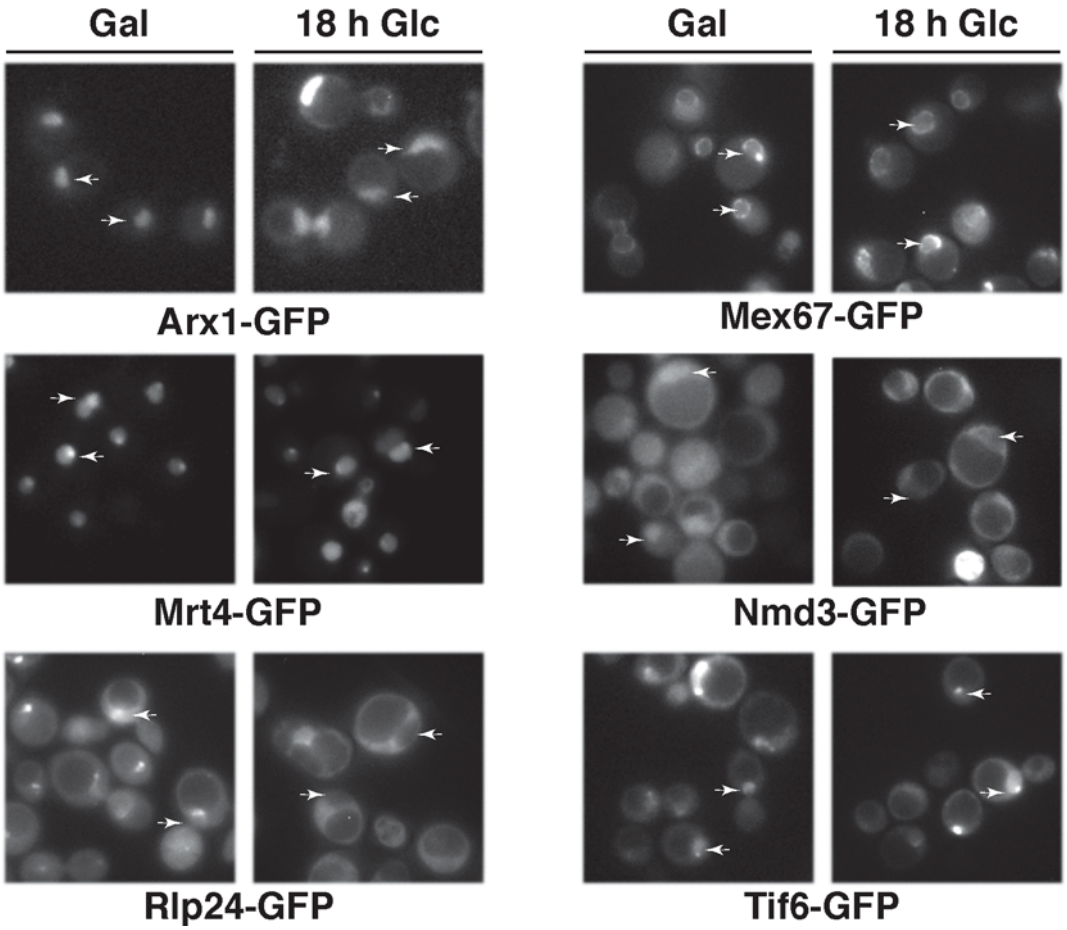

Figure 11- 1 column